



Synthesis and biological activity of fibrate-based acyl- and alkyl-phenoxyacetic methyl esters and 1,2-dihydroquinolines

Abraham Pucheta^{1,2} · Aarón Mendieta^{1,3} · Damián A. Madrigal^{1,2} · Roberto I. Hernández-Benitez¹ · Liseth Romero² · Leticia Garduño-Siciliano² · Catalina Rugerio-Escalona³ · María C. Cruz-López³ · Fabiola Jiménez³ · Alejandra Ramírez-Villalva⁴ · Aydeé Fuentes-Benites⁴ · Carlos González-Romero⁴ · Omar Gómez-García¹ · Julio López⁵ · Miguel A. Vázquez⁵ · Blanca Rosales-Acosta⁶ · Lourdes Villa-Tanaca⁶ · Alfonso Sequeda-Juárez⁷ · Eva Ramón-Gallegos⁷ · Germán Chamorro-Cevallos² · Francisco Delgado¹ · Joaquín Tamariz¹

Received: 10 October 2019 / Accepted: 22 December 2019 / Published online: 26 January 2020
© Springer Science+Business Media, LLC, part of Springer Nature 2020

Abstract

A series of highly potent antihyperlipidemic agents constituted by a fibrate-based structure was recently reported by our group, whose synthesis started from isovanillin derivatives. In the interest of evaluating the bioisosteric effect of the vanillin-based isomers on their antihyperlipidemic activity, the present study focuses on the synthesis of 5-acyl-1-phenoxyacetic methyl esters **5a–c** and their saturated side-chain 5-alkyl-1-phenoxyacetates **6a–c**. Their strong *in vivo* effect was associated with the inhibition of HMG-CoA reductase. Since 1,2-dihydroquinolines inhibit this enzyme, a series of such heterocycles (**9a–d**) was prepared by our efficient regioselective, one-step, solvent-free method. Apart from showing hypolipidemic activity *in vivo*, some of the compounds displayed antifungal, antioxidant and cytotoxic activity *in vitro*. The binding mode of four compounds at the active site of HMGRh was examined with docking simulations, observing an interaction with most of the amino acids targeted by simvastatin.

Keywords Antihyperlipidemic activity · 2-Acyl-1-hydroxyphenoxyacetic esters · 2-Alkyl-1-hydroxyphenoxyacetic esters · 1,2-Dihydroquinolines · HMG-CoA reductase · Antioxidant activity

Supplementary information The online version of this article (<https://doi.org/10.1007/s00044-019-02496-1>) contains supplementary material, which is available to authorized users.

✉ Germán Chamorro-Cevallos
gchamcev@yahoo.com.mx

✉ Joaquín Tamariz
jtamarizm@gmail.com

¹ Departamento de Química Orgánica, Escuela Nacional de Ciencias Biológicas, Instituto Politécnico Nacional (IPN). Prol. Carpio y Plan de Ayala S/N, 11340 Mexico City, Mexico

² Departamento de Farmacia, Escuela Nacional de Ciencias Biológicas, Instituto Politécnico Nacional, Av. Wilfrido Massieu S/N, Unidad Adolfo López Mateos, 07738 Mexico City, Mexico

³ Centro de Investigación en Biotecnología Aplicada, IPN. Carretera Estatal Santa Inés Tecuexcomac-Tepetitla, Km 1.5, Tepetitla de Lardizábal, 90700 Tlaxcala, Mexico

Introduction

Hyperlipidemia, which represent a significant cardiovascular risk factor, is a growing public health problem worldwide (Thagizadeh et al. 2019). It is mainly associated with diseases such as atherosclerosis (Yuan et al. 2007; Steinberg 2005) and ischemic heart disease (Mehta et al.

⁴ Departamento de Química Orgánica, Facultad de Química, Universidad Autónoma del Estado de México (UAEM), Paseo Tollocan y Colón S/N, 50000 Toluca, Mexico

⁵ Departamento de Química, Universidad de Guanajuato, Noria Alta S/N, 36050 Guanajuato, Gto, Mexico

⁶ Laboratorio de Genética Microbiana, Escuela Nacional de Ciencias Biológicas, Instituto Politécnico Nacional, Prol. Carpio y Plan de Ayala S/N, 11340 Mexico City, Mexico

⁷ Departamento de Morfología, Escuela Nacional de Ciencias Biológicas, Instituto Politécnico Nacional, Av. Wilfrido Massieu S/N, Unidad Adolfo López Mateos, 07738 Mexico City, Mexico

2014). Obesity and diabetes may contribute substantially to the elevated prevalence of dyslipidemia (Van Gaal et al. 2006; Aguilar-Salinas et al. 2001). When lifestyle changes (e.g., diet, exercise, and weight loss) fail to control dyslipidemia, healthcare systems turn to the prescription of lipid-lowering medication (Gielen et al. 2009; Grundy et al. 2005). Although many synthetic drugs are available to treat hyperlipidemia, they are related with multiple adverse effects, such as myopathy, rhabdomyolysis, and liver toxicity (Chalasanani 2005; Graham et al. 2004; Elisaf et al. 2008; Hodel 2002; Joy and Hegele 2009; Williams and Feely 2002; Davidson et al. 2007).

Statins are among the most commonly used drugs for the clinical management of hypercholesterolemia (Maron et al. 2000; Wierzbicki 2001; Miyazaki et al. 2004; Vivancos et al. 1999). Their adverse effects include rhabdomyolysis, cognitive decline, neuropathy, pancreatic, and hepatic dysfunction, and an increased risk of cancer (Golomb and Evans 2008; Rotta-Bonfin et al. 2015). The mechanism of their activity has been established as the inhibition of the 3-hydroxy-3-methylglutaryl-coenzyme A (HMG-CoA) reductase (HMGR), an enzyme involved in the biosynthesis of cholesterol (Singh et al. 2009; Haines et al. 2013).

Among other agents inhibiting HMGR (Menéndez et al. 2001; Liu and Yeh 2002; Parker et al. 1993; Sung et al. 2004; Bradfute and Simoni 1994; Harada-Shiba et al. 1995; Panini et al. 1986) are cholestin (Man et al. 2002), diosgenin (Raju and Bird 2007), lanosterol analogs (Trzaskos et al. 1993), β -sitosterol (Field et al. 1997), and the natural product α -asarone (**1**) (active metabolite of the Yucatan peninsula (Mexico) tree called Elemuy (*Mosannonna depressa* (Baill.) Chatrou) (Campos-Ríos and Chiang Cabrera 2006)) resulting in an antihyperlipidemic effect (Chamorro et al. 1993). α -Asarone (**1**) has also been reported to inhibit HMGR (Singh et al. 2009; Rodríguez-Páez et al. 2003) and exhibit antifungal (Momin and Nair 2002; Lee et al. 2004) and antithrombotic (Poplawsky et al. 2000) activity.

Fibrates such as clofibrate (**2a**) (Oliver 2012; Mohamadzadeh et al. 2013), bezafibrate (**2b**) (BIP study group 2000), and fenofibrate (**2c**) (Uchida et al. 2011) are phenoxyacetic-based compounds with a potent hypotriglyceridemic activity (Lalloyer and Staels 2010; Jover-Fernández and Hernández-Mijares 2012). Unlike statins, their mechanism of action consists of binding to and activating peroxisome proliferator activated receptor α (PPAR α), a transcription factor (Schoonjans et al. 1996; Willson et al. 2000; Fazio and Linton 2004; Shaikh and Ali 2018). Fibrates enhance HDL cholesterol but can cause myopathy, cholelithiasis, nausea, syndrome of inappropriate secretion of antidiuretic hormone ADH (SIADH), and liver injury (The Field Study 2005; Okopień et al. 2018). These adverse side effects were among other motives that

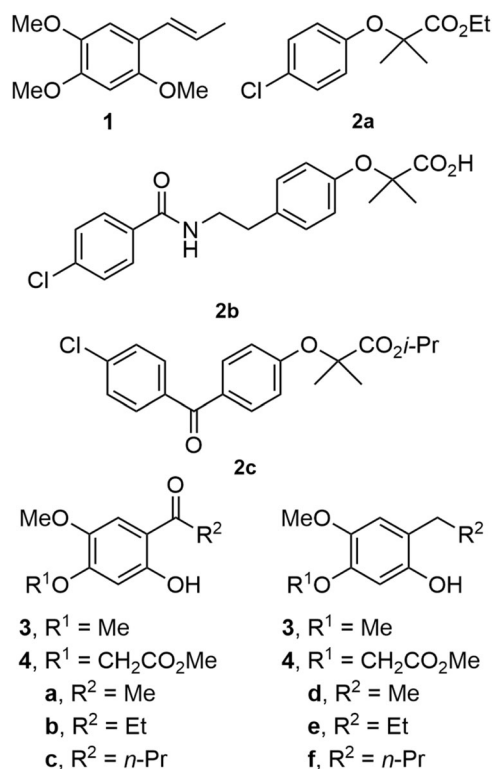


Fig. 1 Structures of α -asarone (**1**), clofibrate (**2a**), bezafibrate (**2b**), fenofibrate (**2c**), α -asarone analogs **3a–f**, and fibrate analogs **4a–f**

clofibrate was withdrawn from the market in some countries. The biological activity of phenoxy acids and their derivatives is exceptionally wide-ranging, being antihyperlipidemic, hypoglycemic, antimicrobial, antiviral, antitubercular, anti-inflammatory, analgesic, antioxidant, anticancer, and anti-hypertensive (Shaheen et al. 2016).

In the search of new synthetic hypolipidemic agents with fewer or no side effects, our group previously synthesized a series of α -asarone (**1**) analogs that showed the desired activity in potent form (Argüelles et al. 2010; Cruz et al. 2003). Docking studies revealed the binding mode of **1** with the active site of the human HMGR (HMGRh) enzyme (Medina-Franco et al. 2005). Moreover, the oxyacetic group at the C-2 position of **1** (Argüelles et al. 2010), mimicking the fibrate structure, proved to have a significant lipid-lowering activity (Labarrios et al. 1999; Zúñiga et al. 2005). Particularly, the series of α -asarone- **3a–f** and phenoxyacetic-based derivatives **4a–f** (Fig. 1) (all prepared from isovanillin) displayed a sharp reduction in cholesterol, LDL-cholesterol, and triglycerides, indicating HMGRh inhibition (Mendieta et al. 2014).

On the other hand, there is evidence of diverse types of biological activity of 1,2-dihydroquinolines, found to act as antidiabetic, anti-inflammatory (Hegedüs et al. 2007), antibacterial (Johnson et al. 1989), antioxidant and cytotoxic (Dorey et al. 2000; Błaszczuk and Skolimowski 2007; Błaszczuk et al. 2013; de Koning 2002) (Błaszczuk et al.

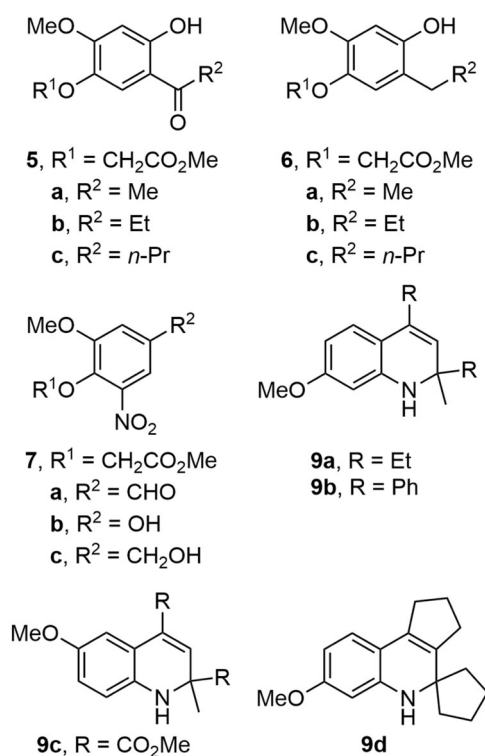


Fig. 2 Structures of the synthesized fibrate-based analogs **5a–c**, **6a–c**, and **7a–c**, and the 1,2-dihydroquinolines **9a–d**

2006; Błaszczuk and Skolimowski 2005; Błaszczuk and Skolimowski 2006) agents. Likewise, analogous 1,2,3,4-tetrahydroquinolines have shown antifungal (Chander et al. 2016a), antimicrobial (Chander et al. 2016b), and antioxidant (Dorey et al. 2000) activity, which has been associated with their capacity of lipid peroxidation and the inhibition of HMGR (Hegedüs et al. 2007). Consequently, these heterocycles may also produce a general hypolipidemic, antioxidant and antifungal effect.

The first aim of the present study was to examine the possible impact on the antihyperlipidemic activity caused by the isomeric position of the substituents in the benzene ring of vanillin-based isomers. Thus, three series of fibrate-based compounds were synthesized starting from vanillin (**8**) and their structure elucidated. The series consisted of 5-acyl-1-phenoxyacetic methyl esters **5a–c**, their saturated side-chain 5-alkyl-1-phenoxyacetates **6a–c** and nitrophenoxyacetates **7a–c** (Fig. 2). Due to the HMGR-related activity of hydroquinolines, a series of the latter was synthesized by using our regioselective one-step method (Gutiérrez et al. 2013). These compounds, **9a–d**, were evaluated *in vivo* as hypolipidemic agents, and *in vitro* for their antifungal, antioxidant, and anticancer effect. The mechanism of action of the test compounds on the HMGRh structure was explored with docking simulations.

Materials and methods

Chemistry

Melting points were determined with an Electrothermal capillary melting point apparatus. IR spectra were recorded on an FT-IR Perkin Elmer 2000 spectrophotometer. ¹H (300 or 500 MHz) and ¹³C (75.4 or 125 MHz) NMR spectra were recorded on Varian Mercury-300 or Varian VNMR System instruments, with TMS as internal standard. Mass spectra (MS) were taken in the electron impact (EI) mode on Hewlett-Packard 5971A and Thermo-Finnigan Polaris Q spectrometers. High-resolution mass spectra (HRMS) were obtained (EI) on a Jeol JSM-GCMateII spectrometer. Commercial reagents were used as received from Aldrich and anhydrous solvents were obtained by a distillation process. Thin layer chromatography was performed on precoated silica gel plates (Merck 60F₂₅₄). Silica gel (230–400 mesh) was used for column chromatography. All air moisture sensitive reactions were carried out with oven-dried glassware under nitrogen atmosphere. Prior to use, acetone and DMF were distilled from 4Å; molecular sieves and methylene chloride from calcium hydride. K₂CO₃ was dried overnight at 120 °C before use. All other reagents were used without further purification. The preparation of compounds **12** (Grenier et al. 2000; Kiss et al. 2010; Rashid et al. 2018) and **9a–d** has been previously described (Gutiérrez et al. 2013).

Methyl 2-(4-formyl-2-methoxyphenoxy)acetate (**10**)

Under an N₂ atmosphere, a mixture of vanillin (**8**) (10.00 g, 65.72 mmol), methyl bromoacetate (16.463 g, 98.58 mmol), and dry K₂CO₃ (18.165 g, 131.44 mmol) in anhydrous acetone (100 mL) was heated to 60 °C for 4 h. The reaction mixture was filtered and the solvent removed under vacuum. The residue was purified by column chromatography over silica gel (20 g/g of crude, hexane/EtOAc, 8:2) to give **10** (13.41 g, 91%) as a white solid. *R*_f 0.48 (hexane/EtOAc, 6:4); m.p. 92–93 °C. IR (KBr): $\bar{\nu}$ 2994, 1740, 1677, 1591, 1508, 1452, 1404, 1285, 1261, 1224, 1136, 1028, 861, 807, 735 cm⁻¹. ¹H NMR (500 MHz, CDCl₃): δ 3.81 (s, 3H, CO₂CH₃), 3.96 (s, 3H, OCH₃), 4.80 (s, 2H, CH₂CO₂CH₃), 6.89 (d, *J* = 8.5 Hz, 1H, H-6'), 7.42 (dd, *J* = 8.5, 1.8 Hz, 1H, H-5'), 7.44 (d, *J* = 1.8 Hz, 1H, H-3'), 9.87 (s, 1H, CHO). ¹³C NMR (125 MHz, CDCl₃): δ 52.4 (CO₂CH₃), 56.0 (OCH₃), 65.8 (CH₂CO₂CH₃), 109.8 (C-3'), 112.3 (C-6'), 126.1 (C-5'), 131.2 (C-4'), 149.9 (C-2'), 152.4 (C-1'), 168.5 (CO₂CH₃), 190.7 (CHO). MS (70 eV): *m/z* 224 (M⁺, 100), 165 (25), 150 (30), 137 (35), 119 (36), 105 (20), 95 (30), 77 (31), 59 (32). HRMS (EI): calcd. for C₁₁H₁₂O₅ [M]⁺ 224.0685; found: 224.0685.

Methyl 2-(4-hydroxy-2-methoxyphenoxy)acetate (11)

A mixture of **10** (10,000 g, 44.64 mmol) and *m*CPBA (77%) (15,000 g, 66.96 mmol) in CH₂Cl₂ (100 mL) was stirred at room temperature (rt) for 12 h. The solvent was removed under vacuum, and MeOH (100 mL) and HCl (6N) (5 mL) were added. The reaction mixture was stirred at rt for 1 h before removing the solvent under vacuum. A saturated aqueous solution of NaHCO₃ was added until neutral, then extracted with EtOAc (4 × 50 mL). The organic layer was dried (Na₂SO₄) and the solvent removed under vacuum. The residue was purified by column chromatography over silica gel (20 g/g of crude, hexane/EtOAc, 7:3) to afford **11** (6.814 g, 72%) as a white solid. *R*_f 0.43 (hexane/EtOAc, 6:4); m.p. 89–90 °C. IR (KBr): $\bar{\nu}$ 3431, 2958, 1732, 1612, 1512, 1479, 1433, 1309, 1208, 1136, 1081, 1032, 953, 837, 793, 766, 712 cm⁻¹. ¹H NMR (300 MHz, CDCl₃): δ 3.79 (s, 3H, CO₂CH₃), 3.80 (s, 3H, OCH₃), 4.62 (s, 2H, CH₂CO₂CH₃), 4.96 (br, 1H, OH), 6.30 (dd, *J* = 8.5, 2.7 Hz, 1H, H-5'), 6.46 (d, *J* = 2.7 Hz, 1H, H-3'), 6.75 (d, *J* = 8.5 Hz, 1H, H-6'). ¹³C NMR (75 MHz, CDCl₃): δ 52.2 (CO₂CH₃), 55.7 (OCH₃), 67.6 (CH₂CO₂CH₃), 100.7 (C-3'), 106.0 (C-5'), 116.7 (C-6'), 140.9 (C-1'), 150.7 (C-2'), 151.8 (C-4'), 170.2 (CO₂CH₃). HRMS (EI): calcd. for C₁₀H₁₂O₅ [M]⁺ 212.0685; found: 212.0681.

General procedure for preparing 5-acylphenoxyacetic methyl esters 5a–c

Under an N₂ atmosphere and at rt, a mixture of **11** (1.0 mol equiv.) and of the respective acyl chloride (1.5 mol equiv.) was stirred for 10 min. Subsequently, BF₃·OEt₂ (1.0 mol equiv.) was added, stirred at rt for 20 min, and then heated to 80 °C for 4 h. Ice was poured into the reaction mixture, followed by adding a saturated aqueous solution of NaHCO₃ dropwise until neutral, then washed with EtOAc (3 × 50 mL). The organic extract was dried (Na₂SO₄) and the solvent removed under vacuum. The residue was purified by column chromatography over silica gel (20 g/g of crude, hexane/EtOAc, 85:15).

Methyl 2-(5-acetyl-4-hydroxy-2-methoxyphenoxy)acetate (5a)

Following the general procedure, **11** (1.000 g, 4.72 mmol) was mixed with acetyl chloride (0.555 g, 7.07 mmol) and BF₃·OEt₂ (0.670 g, 4.72 mmol) to provide **5a** (0.91 g, 76%) as a white solid. *R*_f 0.31 (hexane/EtOAc, 7:3); m.p. 125–126 °C. IR (KBr): $\bar{\nu}$ 3472, 2974, 2372, 1744, 1640, 1614, 1503, 1440, 1365, 1334, 1265, 1202, 1163, 1058, 1007, 975, 814, 710 cm⁻¹. ¹H NMR (500 MHz, CDCl₃): δ 2.53 (s, 3H, CH₃CO), 3.80 (s, 3H, CO₂CH₃), 3.90 (s, 3H,

OCH₃), 4.62 (s, 2H, CH₂CO₂CH₃), 6.46 (s, 1H, H-3'), 7.29 (s, 1H, H-6'), 12.61 (s, 1H, OH). ¹³C NMR (125 MHz, CDCl₃): δ 26.3 (CH₃CO), 52.2 (CO₂CH₃), 56.1 (OCH₃), 68.1 (CH₂CO₂CH₃), 100.9 (C-3'), 111.9 (C-5'), 118.3 (C-6'), 139.6 (C-1'), 157.8 (C-2'), 161.2 (C-4'), 169.5 (CO₂CH₃), 202.2 (CH₃CO). MS (70 eV): *m/z* 254 (M⁺, 51), 239 (6), 195 (7), 181 (100), 153 (14), 135 (15), 107 (9). HRMS (EI): calcd for C₁₂H₁₄O₆ [M]⁺: 254.0790; found: 254.0787.

Methyl 2-(4-hydroxy-2-methoxy-5-propionylphenoxy)acetate (5b)

Following the general procedure, **11** (1.000 g, 4.72 mmol) was mixed with propanoyl chloride (0.654 g, 7.07 mmol) and BF₃·OEt₂ (0.670 g, 4.72 mmol) to obtain **5b** (0.91 g, 76%) as a white solid. *R*_f 0.40 (hexane/EtOAc, 7:3); m.p. 105–106 °C. IR (KBr): $\bar{\nu}$ 3482, 2979, 2942, 1748, 1638, 1616, 1565, 1504, 1439, 1375, 1319, 1249, 1193, 1158, 1069, 1007, 975, 945, 820, 707 cm⁻¹. ¹H NMR (300 MHz, CDCl₃): δ 1.22 (t, *J* = 7.2 Hz, 3H, CH₃CH₂CO), 2.90 (q, *J* = 7.2 Hz, 2H, CH₃CH₂CO), 3.80 (s, 3H, CO₂CH₃), 3.90 (s, 3H, OCH₃), 4.62 (s, 2H, CH₂CO₂CH₃), 6.46 (s, 1H, H-3'), 7.33 (s, 1H, H-6'), 12.70 (s, 1H, OH). ¹³C NMR (75 MHz, CDCl₃): δ 8.3 (CH₃CH₂CO), 31.2 (CH₃CH₂CO), 52.1 (CO₂CH₃), 56.0 (OCH₃), 68.0 (CH₂CO₂CH₃), 100.9 (C-3'), 111.3 (C-5'), 117.5 (C-6'), 139.5 (C-1'), 157.4 (C-2'), 161.1 (C-4'), 169.5 (CO₂CH₃), 204.9 (CH₃CH₂CO). MS (70 eV): *m/z* 268 (M⁺, 66), 239 (66), 195 (100), 138 (22), 121 (14). HRMS (EI): *m/z* calcd for C₁₃H₁₆O₆ [M]⁺: 268.0947; found: 268.0946.

Methyl 2-(5-butyryl-4-hydroxy-2-methoxyphenoxy)acetate (5c)

Following the general procedure, **11** (1.000 g, 4.72 mmol) was mixed with butanoyl chloride (0.753 g, 7.07 mmol) and BF₃·OEt₂ (0.670 g, 4.72 mmol) to produce **5c** (0.892 g, 67%) as a white solid. *R*_f 0.46 (hexane/EtOAc, 7:3); m.p. 82–83 °C. IR (KBr): $\bar{\nu}$ 3482, 2954, 1748, 1637, 1511, 1442, 1384, 1336, 1283, 1253, 1197, 1162, 1075, 1019, 986, 900, 848, 793, 703 cm⁻¹. ¹H NMR (300 MHz, CDCl₃): δ 1.01 (t, *J* = 7.5 Hz, 3H, CH₃(CH₂)₂CO), 1.75 (sext, *J* = 7.5 Hz, 2H, CH₃CH₂CH₂CO), 2.84 (t, *J* = 7.5 Hz, 2H, CH₃CH₂CH₂CO), 3.81 (s, 3H, CO₂CH₃), 3.91 (s, 3H, OCH₃), 4.63 (s, 2H, CH₂CO₂CH₃), 6.46 (s, 1H, H-3'), 7.32 (s, 1H, H-6'), 12.78 (s, 1H, OH). ¹³C NMR (75 MHz, CDCl₃): δ 13.8 (CH₃(CH₂)₂CO), 18.1 (CH₃CH₂CH₂CO), 39.9 (CH₃CH₂CH₂CO), 52.2 (CO₂CH₃), 56.1 (OCH₃), 68.0 (CH₂CO₂CH₃), 100.87 (C-3'), 111.4 (C-5'), 117.5 (C-6'), 139.5 (C-1'), 157.4 (C-2'), 161.2 (C-4'), 169.5 (CO₂CH₃), 204.6 (CH₃(CH₂)₂CO). MS (70 eV): *m/z* 282 (M⁺, 66), 239 (68), 209 (100), 167 (14), 138 (20), 107 (10), 69 (16).

HRMS (EI): m/z calcd for $C_{14}H_{18}O_6$ $[M]^+$: 282.1103; found: 282.1100.

General procedure for preparing 5-alkylphenoxyacetic methyl esters 6a–c

Under an N_2 atmosphere and at rt, a mixture of Zn/Hg and HCl (36%) (1.0 g/1.0 mL, 10.0 mol equiv.) was stirred for 5 min before being poured into a flask. Addition was made of the corresponding acyl derivative **5a–c** (1.0 mol equiv.), followed by a mixture of MeOH/HCl (1.0/0.2 mL). After heating to 60 °C for 4 h, ice was poured in and a saturated aqueous solution of $NaHCO_3$ added dropwise until neutral, and then washed with EtOAc (3 × 30 mL). The organic extract was dried (Na_2SO_4) and the solvent was removed under vacuum. The residue was purified by column chromatography over silica gel (20 g/g of crude, hexane/EtOAc, 95:5).

Methyl 2-(5-ethyl-4-hydroxy-2-methoxyphenoxy)acetate (6a)

Following the general procedure, **5a** (1.000 g, 3.94 mmol) was mixed with Zn/Hg (10.47 g, 39.4 mmol) to furnish **6a** (0.68 g, 72%) as a white solid. R_f 0.26 (hexane/EtOAc, 7:3); m.p. 66–67 °C. IR (KBr): $\bar{\nu}$ 3402, 2961, 2925, 2866, 1750, 1717, 1616, 1525, 1447, 1423, 1367, 1293, 1237, 1204, 1122, 1069, 1007, 857, 747, 706 cm^{-1} . 1H NMR (500 MHz, $CDCl_3$): δ 1.17 (t, $J = 7.5$ Hz, 3H, H-2''), 2.52 (q, $J = 7.5$ Hz, 2H, H-1''), 3.78 (s, 6H, CO_2CH_3 , OCH₃), 4.62 (s, 2H, $CH_2CO_2CH_3$), 4.77–4.84 (m, 1H, OH), 6.42 (s, 1H, H-3'), 6.73 (s, 1H, H-6'). ^{13}C NMR (125 MHz, $CDCl_3$): δ 14.2 (C-2''), 22.3 (C-1''), 52.1 (CO_2CH_3), 55.9 (OCH₃), 68.0 ($CH_2CO_2CH_3$), 101.1 (C-3'), 117.7 (C-6'), 120.9 (C-5'), 141.0 (C-1'), 148.8 (C-2', C-4'), 170.1 (CO_2CH_3). HRMS (EI): m/z calcd for $C_{12}H_{16}O_5$ $[M]^+$: 240.0998; found: 240.1000.

Methyl 2-(4-hydroxy-2-methoxy-5-propylphenoxy)acetate (6b)

Following the general procedure, **5b** (1.000 g, 3.73 mmol) was mixed with Zn/Hg (9.93 g, 37.3 mmol) to form **6b** (0.663 g, 70%) as a white solid. R_f 0.30 (hexane/EtOAc, 7:3); m.p. 54–55 °C. IR (KBr): $\bar{\nu}$ 3390, 3019, 2955, 2867, 1871, 1708, 1619, 1528, 1450, 1419, 1377, 1302, 1198, 1120, 1078, 1008, 884, 866, 843, 768, 739, 703 cm^{-1} . 1H NMR (300 MHz, $CDCl_3$): δ 0.93 (t, $J = 7.4$ Hz, 3H, H-3''), 1.57 (sext, $J = 7.4$ Hz, 2H, H-2''), 2.46 (t, $J = 7.4$ Hz, 2H, H-1''), 3.73 (s, 3H, OCH₃), 3.78 (s, 3H, CO_2CH_3), 4.61 (s, 2H, $CH_2CO_2CH_3$), 5.45 (br s, 1H, OH), 6.42 (s, 1H, H-3'), 6.69 (s, 1H, H-6'). ^{13}C NMR (75 MHz, $CDCl_3$): δ 13.8 (C-3''), 23.0 (C-2''), 31.3 (C-1''), 52.1 (CO_2CH_3), 55.7 (OCH₃),

67.8 ($CH_2CO_2CH_3$), 100.9 (C-3'), 118.1 (C-6'), 119.5 (C-5'), 140.5 (C-1'), 148.5 (C-2'), 149.1 (C-4'), 170.3 (CO_2CH_3). HRMS (EI): m/z calcd for $C_{13}H_{18}O_5$ $[M]^+$: 254.1154; found: 254.1151.

Methyl 2-(5-butyl-4-hydroxy-2-methoxyphenoxy)acetate (6c)

Following the general procedure, **5c** (1.000 g, 3.55 mmol) was mixed with Zn/Hg (9.43 g, 35.5 mmol), resulting in **6c** (0.65 g, 68%) as a white solid. R_f 0.31 (hexane/EtOAc, 7:3); m.p. 49–50 °C. IR (KBr): $\bar{\nu}$ 3448, 3019, 2952, 2860, 1719, 1617, 1529, 1449, 1417, 1367, 1306, 1206, 1123, 1078, 1013, 939, 894, 856, 829, 759, 714 cm^{-1} . 1H NMR (500 MHz, $CDCl_3$): δ 0.94 (t, $J = 7.5$ Hz, 3H, H-4''), 1.35 (sext, $J = 7.5$ Hz, 2H, H-3''), 1.53 (qu, $J = 7.5$ Hz, 2H, H-2''), 2.45 (t, $J = 7.5$ Hz, 2H, H-1''), 3.79 (s, 3H, CO_2CH_3), 3.80 (s, OCH₃), 4.61 (s, 2H, $CH_2CO_2CH_3$), 6.42 (s, 1H, H-3'), 6.70 (s, 1H, H-6'). ^{13}C NMR (125 MHz, $CDCl_3$): δ 13.9 (C-4''), 22.4 (C-3''), 29.0 (C-1''), 32.1 (C-2''), 52.1 (CO_2CH_3), 56.0 (OCH₃), 68.0 ($CH_2CO_2CH_3$), 101.1 (C-3'), 118.4 (C-6'), 119.4 (C-5'), 141.0 (C-1'), 148.9 (C-2', C-4'), 170.0 (CO_2CH_3). HRMS (EI): m/z calcd for $C_{14}H_{20}O_5$ $[M]^+$: 268.1311; found: 268.1303.

Methyl 2-(4-Formyl-2-methoxy-6-nitrophenoxy)acetate (7a)

Under N_2 atmosphere, a mixture of **12** (10.000 g, 50.76 mmol), dry K_2CO_3 (14.010 g, 101.52 mmol) and methyl bromoacetate (15.10 g, 98.7 mmol) in anhydrous DMF (50 mL) was stirred at 60 °C for 4 h (Brown et al. 2010). The reaction mixture was filtered, the solvent removed under vacuum, and the residue purified by column chromatography over silica gel (20 g/g of crude, hexane/EtOAc, 8:2) to give **7a** (9150 g, 67%) as a yellow solid. R_f 0.66 (hexane/EtOAc, 1:1); m.p. 96–97 °C. IR (KBr): $\bar{\nu}$ 3385, 3086, 3014, 2956, 2851, 1752, 1701, 1604, 1541, 1466, 1427, 1357, 1289, 1218, 1202, 1141, 1046, 918, 872, 772, 680 cm^{-1} . 1H NMR (300 MHz, $CDCl_3$): δ 3.78 (s, 3H, CO_2CH_3), 3.99 (s, 3H, OCH₃), 4.90 (s, 2H, $CH_2CO_2CH_3$), 7.64 (d, $J = 1.8$ Hz, 1H, H-3'), 7.88 (d, $J = 1.8$ Hz, 1H, H-5'), 9.93 (s, 1H, CHO). ^{13}C NMR (75 MHz, $CDCl_3$): δ 52.3 (CO_2CH_3), 56.8 (OCH₃), 69.4 ($CH_2CO_2CH_3$), 113.5 (C-3'), 119.7 (C-5'), 131.7 (C-4'), 145.2 (C-1'), 153.6 (C-2'), 168.5 (CO_2CH_3), 188.9 (CHO). HRMS (EI): m/z calcd for $C_{11}H_{11}NO_7$ $[M]^+$: 269.0535; found: 269.0541.

Methyl 2-(4-hydroxy-2-methoxy-6-nitrophenoxy)acetate (7b)

A mixture of **7a** (1.000 g, 3.72 mmol) and *m*CPBA (77%) (1.240 g, 5.57 mmol) in CH_2Cl_2 (10 mL) was stirred at rt for 4 h before removing the solvent under vacuum. MeOH

(10 mL) and HCl (37%) (1 mL) were added, the mixture was stirred at rt for 2 h, and the solvent was removed under vacuum. An aqueous saturated solution of NaHCO₃ was added until neutral, then extracted with EtOAc (4 × 50 mL). The organic layer was dried (Na₂SO₄), the solvent removed under vacuum, and the residue purified by column chromatography over silica gel (20 g/g of crude, hexane/EtOAc, 1:1) to afford **7b** (0.580 g, 61%) as a pale yellow solid. *R_f* 0.33 (EtOAc); m.p. 110–111 °C. IR (KBr): $\bar{\nu}$ 3070, 2952, 2643, 1732, 1609, 1542, 1490, 1466, 1421, 1354, 1289, 1222, 1202, 1114, 1066, 1017, 918, 897, 865, 854, 814, 775, 755, 736, 700 cm⁻¹. ¹H NMR (500 MHz, CDCl₃): δ 3.79 (s, 3H, CO₂CH₃), 3.99 (s, 3H, OCH₃), 4.89 (s, 2H, CH₂CO₂CH₃), 7.80 (d, *J* = 2.0 Hz, 1H, H-3'), 8.12 (d, *J* = 2.0 Hz, 1H, H-5'). ¹³C NMR (125 MHz, CDCl₃): δ 52.3 (CO₂CH₃), 56.8 (OCH₃), 69.5 (CH₂CO₂CH₃), 116.8 (C-3'), 118.7 (C-5'), 124.6 (C-6'), 144.6 (C-1'), 153.0 (C-2'), 168.6 (CO₂CH₃), 169.1 (C-4'). HRMS (EI): *m/z* calcd for C₁₀H₁₁NO₇ [M]⁺: 257.0536; found: 257.0531.

Methyl 2-(4-(hydroxymethyl)-2-methoxy-6-nitrophenoxy) acetate (**7c**)

Under N₂ atmosphere and at 0 °C, a mixture of **7a** (1.000 g, 3.71 mmol) and NaBH₄ (0.070 g, 1.85 mmol) in MeOH (10 mL) was stirred for 2 h before removing the solvent under vacuum. The residue was purified by column chromatography over silica gel (20 g/g of crude, hexane/EtOAc, 1:1) to provide **7c** (0.86 g, 86%) as a white solid. *R_f* 0.16 (hexane/EtOAc, 1:1); m.p. 97–98 °C. IR (KBr): $\bar{\nu}$ 3481, 2921, 1747, 1535, 1452, 1390, 1355, 1276, 1241, 1208, 1135, 1062, 972, 919, 850, 810, 780 cm⁻¹. ¹H NMR (500 MHz, CDCl₃): δ 2.47 (br, 1H, OH), 3.79 (s, 3H, CO₂CH₃), 3.90 (s, 3H, OCH₃), 4.68 (s, 2H, CH₂OH), 4.73 (s, 2H, CH₂CO₂CH₃), 7.14 (d, *J* = 1.5 Hz, 1H, H-3'), 7.29 (d, *J* = 1.5 Hz, 1H, H-5'). ¹³C NMR (125 MHz, CDCl₃): δ 52.2 (CO₂CH₃), 56.4 (OCH₃), 63.7 (CH₂OH), 69.6 (CH₂CO₂CH₃), 113.7 (C-5'), 114.2 (C-3'), 138.1 (C-4'), 139.2 (C-1'), 144.5 (C-6'), 153.3 (C-2'), 169.1 (CO₂CH₃). HRMS (EI): *m/z* calcd for C₁₁H₁₃NO₇: 271.0692; found: 271.0687.

Hypolipidemic activity

The hypolipidemic effect of the compounds was studied on male ICR mice weighing 25–30 g (Birmex, Mexico City), which were housed in hanging metal cages and maintained at 24 ± 2 °C and 50 ± 10% relative humidity on a 12 h light/dark cycle (lights on at 8:00 a.m.). Food (a standard pellet diet, Rodent Diet 5001, PMI Nutrition International, Brentwood, MO) and water were freely available. All animals appeared healthy throughout the dosing period, maintaining normal food intake and weight gain. Post-sacrifice analysis

showed no gross abnormalities in any treated mice. All animals were handled and maintained in accordance with ethical principles and regulations specified by the Animal Care and Use Committee of our institution and the standards of the National Institutes of Health of Mexico.

An aqueous solution of Triton WR 1339 was administered intraperitoneally (ip) to mice (400 mg/kg) and after 1 h the test compounds (25, 50, or 100 mg/kg, dissolved in saline, or saline-Tween) were injected ip. Blood was taken from a retro-orbital puncture 24 h later, and the plasma levels of total cholesterol (TC) and triglycerides (TG) were determined in duplicate with commercially available kits. Values are expressed as the mean from 6 animals per compound.

Antifungal activity

The in vitro antimicrobial effect of compounds **5a–c**, **6a–b**, **7a**, **7c**, and **9a–d** was evaluated with susceptibility assays based on the microdilution techniques of the Antimicrobial Susceptibility Testing Protocols standardized by the Clinical and Laboratory Standards Institute (CLSI). The M38-A2 method was used for the four strains of filamentous fungi (CLSI 2002; Espinel-Ingroff and Canton 2007a): *Aspergillus fumigatus* ATCC-16907, *Trichosporon cutaneum* ATCC-28592, *Rhizopus oryzae* ATCC-10329 and *Mucor hiemalis* ATCC-8690. The M27-A3 method was applied for the three strains of ATCC *Candida* yeasts (CLSI 2008; Espinel-Ingroff and Cantón 2007b; Pfaller and Diekema 2012): *C. albicans* ATCC-10231, *C. utilis* ATCC-9226 and *C. tropicalis* ATCC-13803. The test compounds were soluble in dimethyl sulfoxide (DMSO), in accordance with the Antimicrobial Susceptibility Testing Protocols. Hence, the antifungal assays were performed with this solvent.

The minimum inhibitory concentration (MIC) of all compounds and the reference drug (itraconazole), expressed in µg/mL, was determined in 96-well plates, utilizing RPMI-1640 culture medium buffered with 3-(*N*-morpholino)propanesulfonic acid (MOPS, Sigma) and dilutions of 16 to 0.03 µg/mL (according to the procedure outlined in the instructions for each type of fungus).

The inoculum for the yeasts was prepared with culture colonies of 24-h growth strain in SDA medium and resuspending them in a tube of saline solution (0.85% NaCl) to obtain a concentration of ~1–5 × 10⁶ CFU/mL. The necessary amount of saline solution was added to adjust the optical density to 0.5 McFarland. Subsequently, a 1:1000 dilution was made with RPMI medium. For filamentous fungi, the inoculum was elaborated from a culture having undergone 7 days of growth at 35 °C on PDA agar, a medium that induces the formation of conidia or sporangiospores. To remove the conidia, the culture was

introduced and handled in Tween 20, then resuspended in saline solution. The particles were allowed to settle for 5 min, the supernatant transferred to another tube and shaken vigorously for 15 s. Because the size of the conidia is different for each species, the optical density required to reach a concentration of $1\text{--}5 \times 10^6$ CFU/mL varied. Adjustment to the desired value was accomplished with the McFarland Turbidity Standard No. 0.15, based on the methods of the CLSI.

Compounds **5–7** and **9** were prepared (at 10 mM) and tested for their inhibition of *Fusarium oxysporum* with the PDA dilution method (Lalitha 2004). Briefly, PDA medium was sterilized in an autoclave at 121 °C for 20 min, followed by the addition of one of the compounds diluted in DMSO (2%). The plates were inoculated with *F. oxysporum* and then incubated at 26–28 °C for 72 h. All experiments were carried out in triplicates ($n = 12$), and the data are expressed as the mean. The growth inhibition efficiency of each compound was compared with captan (10 mM), the reference drug, and validated by ANOVA and the Tukey test ($p < 0.05$) on the SAS V9.0 program (SAS 2014).

Cytotoxic activity

Cell culture

Cell lines of human cervical cancer (HeLa), prostate cancer (DU-145), breast cancer (MDA-231), and no tumoral cell line (HaCaT) were cultivated in Dulbecco's Minimum Essential Medium (DMEM) containing 10% fetal bovine serum (FBS) and 1% penicillin/streptomycin (100/100 U/mL). Cells were cultured as adherent monolayers and maintained at 37 °C and 5% humidity (Freshney 2010).

Cell viability assay

Cell viability was determined by an MTT (3-[4,5-dimethylthiazol-2-yl]-2,5-diphenyltetrazolium bromide) assay. Cells were harvested, counted, and transferred to 96-well plates at 3000 cells per well to be incubated for 24 h. Upon completion of this time, cells were treated with compounds **5a–b**, **6a–b**, and **9a–c** at concentrations of 10, 20, 40, 60, 80, and 100 µg/mL with 1% DMSO in cell culture medium, then again incubated for 24 h. Subsequently, microscope images were obtained for each cell line exposed to each compound. Cells without treatment were used as the viability control, 1% DMSO as the vehicle control, and methotrexate as the control for comparison of the respective median lethal concentrations (LC₅₀).

In each well, 50 µL of a solution of MTT in culture medium (100 µg/µL) were added and cells were incubated at 37 °C for 4 h. The culture medium was removed and 100 µL of isopropanol was added to each well. Optical density in

each well was measured on an ELISA microplate reader at 595 nm. The result was expressed as the percentage of the viability of control cells and the LC₅₀ was calculated (van Meerloo et al. 2011).

Data analysis

Data analysis was carried out by nonparametric one-way ANOVA and a post hoc with Dunn's test, run on Sigma Plot software version 12 (Motulsky 1999). All data are expressed as the mean ± SD, with significance set at $p < 0.05$. Each experiment was performed in triplicate.

Antioxidant activity

DPPH radical scavenging assay

The scavenging of free radicals by the chromones was assessed by using the 2,2-diphenyl-1-picrylhydrazyl radical (DPPH[•]) assay, as previously described (Cevallos-Casals and Cisneros-Zevallos 2003) with slight modifications. A concentration of 10 mM of each compound was prepared, to which a solution of DPPH[•] (133.33 µM) was added at a ratio of 1:3 (v/v). The mixture was incubated at 37 °C for 30 min and read at 517 nm. Scavenging capacity (SC) was expressed as the percentage decrease in DPPH at 10 mM:

$$SC\% = [(A_{\text{control}} - A_{\text{test}}) / A_{\text{control}}] \times 100$$

where A_{control} is the absorbance of the DPPH solution (control) and A_{test} is the absorbance of the DPPH solution plus a compound.

ABTS radical activity

The free radical scavenging capacity was quantified based on a slightly modified version of the previously reported 2,2'-azino-bis(3-ethylbenzothiazoline-6-sulphonic acid) radical cation (ABTS^{•+}) assay (Gallardo et al. 2016; Zhang et al. 2013). The radical cation was prepared by dissolving the stock solution of ABTS (7 mM in distilled water) with K₂S₂O₈ solution (2.45 mM) at ratio of 1:1 (v/v) and then leaving the mixture to stand in the dark at rt for 16 h. For the evaluation of antioxidant activity, the ABTS^{•+} solution was diluted with absolute ethanol until reaching the absorbency of 0.700 ± 0.02 at 734 nm. Taking 10 µL of the resulting solution at different concentrations (10, 1.0 and 0.1 mM), 1 mL of ABTS solution was added and after 6 min absorbance was read at 734 nm. All tests were performed in triplicate and the mean was centered. Finally, the percentage inhibition of ABTS absorbance was calculated by the aforementioned formula for the DPPH[•] assay. The data are expressed as Trolox equivalent antioxidant capacity (TEAC), developing a standard curve in a range of 0.5 to 3.5 mM.

Molecular docking study

Protein and ligand structures

The crystallographic structures of human HMGRh in complex with a selective inhibitor (simvastatin) were retrieved from the protein data bank (PDB) (<http://www.rcsb.org/>) with the code 1HW9 (Istvan and Deisenhofer 2001). Before docking simulations were run, the coordinates of the protein were set, water molecules removed, hydrogen atoms added to the polar atoms (considering pH at 7.4), and Kollman charges assigned. The 3D structures of simvastatin were downloaded from the Zinc database (Irwin and Shoichet 2005). The structures of the ligands were sketched in 2D with ChemSketch (<https://www.acdlabs.com/resources/freeware/chemsketch/>) and optimized with AM1 on Gaussian 98 software (Frisch et al. 2004) to obtain the minimum energy conformation for docking studies.

Molecular docking

The protein-ligand interaction was observed on Autodock version 4.0 and AutoDockTools (Morris et al. 2009). All the possible rotatable bonds, torsion angles, atomic partial charges and non-polar hydrogens were determined for each ligand. For HMGRh, the grid dimensions in AutoDockTools were $62 \times 82 \times 106 \text{ \AA}^3$ with points separated by 0.375 \AA , centered at $X = 5.564$, $Y = -6.681$, and $Z = 4.637$. The hybrid Lamarckian Genetic Algorithm was applied for minimization, utilizing default parameters. A total of one hundred docking runs were conducted, adopting the conformation with the lowest binding energy (kcal/mol) for all further simulations. The script and files were prepared and the docking results visualized on AutoDockTools, then edited in Discovery 4.0 Client (Dassault Systèmes 2016).

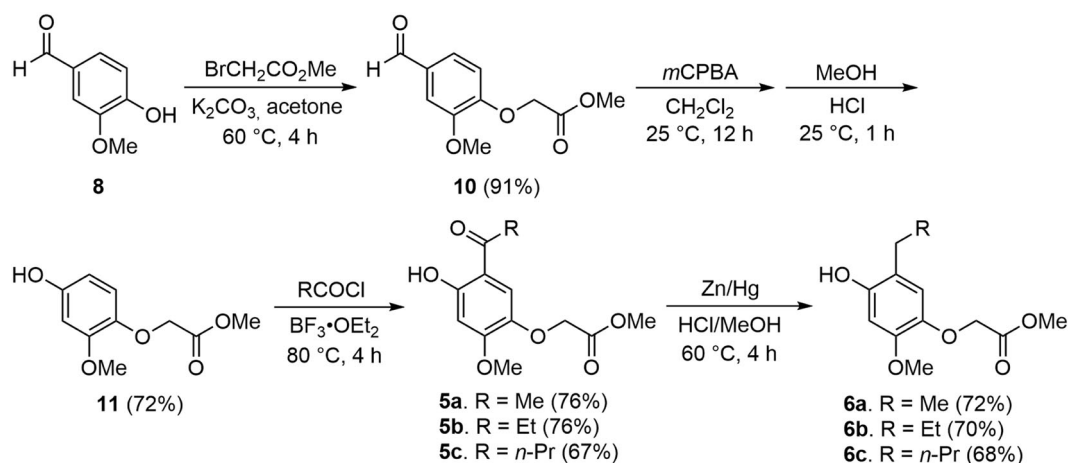
Results and discussion

Chemistry

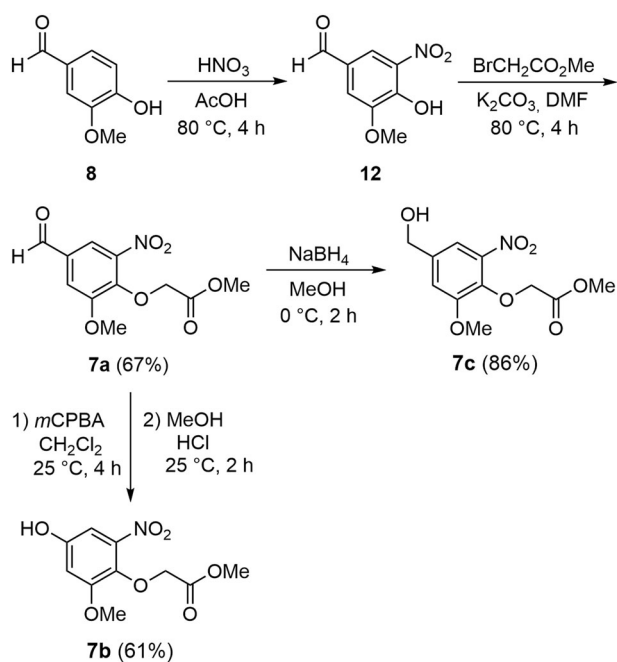
The synthesis of the series of methyl phenoxyacetates **5a–c** and **6a–c** was based on the functionalization of vanillin (**8**) as the starting material (Scheme 1). Firstly, the hydroxy group was protected by the acetate moiety through a Williamson alkylation with methyl bromoacetate under basic conditions (Argüelles et al. 2010) to give compound **10** in high yield. The conversion of the formyl group to the hydroxy group was carried out by a Baeyer–Villiger rearrangement with *m*CPBA, followed by hydrolysis of the formyl ester to furnish the corresponding acylphenoxyacetic esters **5a–c** in fairly good yields (Scheme 1). Conversion of this series into the alkylphenoxyacetic esters **6a–c** took place through a Clemmensen reduction to provide the expected products in good yields.

The structures of all compounds were established by ^1H NMR, ^{13}C NMR, and HRMS. The full assignment of proton and carbon signals was achieved by 2D NMR experiments (HMQC and HMBC). The selective formation of the tetrasubstituted benzene ring was ascertained by the two characteristic singlets for the *para* aromatic protons. The presence of the carbonyl group of the series of acyl derivatives **5a–c** was verified by the signal appearing at around 204 ppm in the ^{13}C NMR spectra.

The series of nitro compounds **7a–c** was readily prepared by direct nitration of vanillin (**8**) to provide the known 5-nitrovanillin (**12**) (Grenier et al. 2000; Kiss et al. 2010;



Scheme 1 Synthesis of phenol **10**, acyl phenols **5a–c**, and alkyl phenols **6a–c**



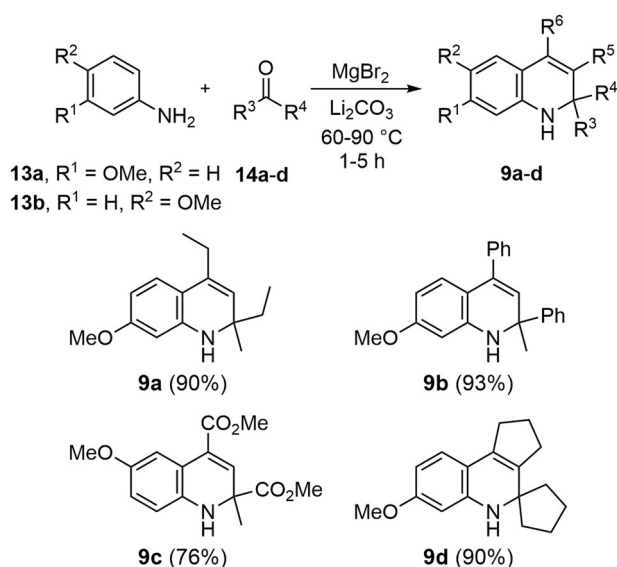
Scheme 2 Synthesis of methyl nitrophenoxyacetates **7a-c** from vanillin (**8**)

Rashid et al. 2018) (Scheme 2). The latter was treated with methyl bromoacetate under basic conditions to obtain the nitrophenoxyacetate **7a** in a 67% yield for the two steps. Baeyer–Villiger rearrangement produced the respective formate, which was hydrolyzed under acid conditions to deliver **7b** in 61% yield. Moreover, reduction of the formyl group of **7a** with sodium borohydride resulted in the hydroxymethyl derivative **7c** in 86% yield.

The synthesis of 1,2-dihydroquinolines **9a-d** was achieved through a single-step reaction, according to the published procedure (Gutiérrez et al. 2013) (Scheme 3). Thus, analogs **9a-b** were prepared in high yields by reacting *m*-anisidine (**13a**) with ketones **14a-b**, under solvent-free conditions and in the presence of magnesium bromide as the catalyst and lithium carbonate as the base. Meanwhile, 1,2-dihydroquinoline **9c** was formed by using *p*-anisidine (**13b**) and methyl pyruvate (**14c**) under similar reaction conditions. Finally, the spiro-polycyclic 1,2-dihydroquinoline **9d** was furnished in high yield via the reaction of **13a** with cyclopentanone (**14d**). The physical data and NMR spectra of the resulting 1,2-dihydroquinolines were in agreement with the previous report (Gutiérrez et al. 2013).

Hypolipidemic activity

The *in vivo* hypolipidemic screening of the compounds **5a-c**, **6a-c**, **7a**, and **9a-d** was performed on male ICR mice subjected to tyloxapol-induced hyperlipidemia (Silva et al. 2001; Kourounakis et al. 2002). The possible mechanism of lipid-lowering agents is commonly evaluated with Triton WR 1339



Scheme 3 Synthesis of 1,2-dihydroquinolines **9a-d**

(tyloxapol), a non-ionic surfactant (Levine and Saltzman 2007; Zeniya and Reuben 1988; Edelstein et al. 1985). It causes a drastic rise in serum triglycerides and cholesterol levels by increasing HMGR activity (Kuroda et al. 1977; Goldfard 1978). To diminish the concentration of blood serum lipids, it is necessary to inhibit the synthesis of endogenous cholesterol (elevated after treatment with tyloxapol), limit the absorption of lipoprotein lipids, and stimulate the excretion of the latter (Korolenko et al. 2010). Many clinically used drugs accomplish some of these functions, such as ezetimibe (inhibitor of cholesterol absorption), fibrates (PPAR- α agonists) and statins (HMGR inhibitors).

The series of analogs **5a-c**, **6a-c**, **7a**, and **9a-d** were administered *ip* at doses of 25, 50, and 100 mg/kg to hyperlipidemic mice, and their effect on the plasma levels (mg/dL) of total cholesterol, and triglycerides was examined with a procedure similar to that employed in previous studies with related compounds (Argüelles et al. 2010). Since preliminary assays showed a very modest decrease in cholesterol by **7a-c**, and considering that the nitro group can be cytotoxic (Chung et al. 2011; Olender et al. 2018), only **7a** was subjected to further assessment of hypolipidemic activity.

All compounds evaluated, including the reference (simvastatin), sharply depleted plasma levels of cholesterol and triglycerides, in the range of 44–75% and 51–93%, respectively, vs. the hyperlipidemic control animals. A significant difference existed between the values of the control and most treatments (Table 1). Moreover, it is worth noticing that almost all compounds significantly decrease triglyceride levels, since it is critical to diminish the concentration of the latter because in excess they induce the formation of atheroma, leading to an imminent cardiovascular disease (Veseli et al. 2017).

Table 1 Effect of the test compounds on the serum lipid profile of male ICR mice^a

Compound	Dose mg/ Kg/day	Cholesterol	Triglycerides
Normal diet		-78.15 ± 0.07*	-80.02 ± 0.08*
Simvastatin	17	-76.38 ± 0.19*	-79.10 ± 0.17*
Tyloxapol	400	100 ± 1.03 ^b	100 ± 0.33 ^c
5a + Tyloxapol	25	-67.29 ± 6.78*	-83.74 ± 2.44*
	50	-75.44 ± 6.27*	-93.40 ± 1.25*
	100	-58.5 ± 7.35*	-86.46 ± 2.31*
5b + Tyloxapol	25	-75.20 ± 3.52*	-81.42 ± 2.51*
	50	-57.49 ± 7.74*	-87.49 ± 1.25*
	100	-52.53 ± 11.61*	-88.95 ± 1.31*
5c + Tyloxapol	25	-73.43 ± 4.70*	-92.04 ± 2.51*
	50	-64.93 ± 11.06*	-91.4 ± 1.79*
	100	-74.02 ± 5.14*	-85.70 ± 1.84*
6a + Tyloxapol	25	-72.84 ± 0.25*	-20.77 ± 0.79
	50	-74.73 ± 0.09*	-80.59 ± 0.11*
	100	-65.40 ± 0.69*	-73.95 ± 0.38*
6b + Tyloxapol	25	-69.89 ± 0.49*	4.11 ± 1.14
	50	-61.03 ± 0.60*	4.11 ± 2.18
	100	-70.89 ± 0.58*	-9.55 ± 0.83
6c + Tyloxapol	25	-71.07 ± 0.70*	-76.25 ± 0.34
	50	-69.30 ± 0.30*	-75.72 ± 0.19*
	100	-72.72 ± 0.41*	-78.22 ± 0.29*
7a + tyloxapol	25	-58.43 ± 0.53	-67.13 ± 0.40*
	50	-59.03 ± 0.78	-66.98 ± 0.60*
	100	-17.46 ± 2.68	-43.01 ± 0.37
9a + tyloxapol	25	-72.27 ± 0.11*	-76.22 ± 0.24*
	50	-63.16 ± 0.62*	-63.26 ± 0.62*
	100	-72.72 ± 0.24*	-70.47 ± 0.44*
9b + tyloxapol	25	-68.82 ± 0.29*	-67.37 ± 0.55*
	50	-44.98 ± 1.45*	-34.11 ± 0.54
	100	-73.78 ± 0.33*	-75.25 ± 0.22*
9c + tyloxapol	25	-51.70 ± 1.01	-60.13 ± 0.46*
	50	28.22 ± 7.82	-66.94 ± 0.57*
	100	-65.99 ± 0.4	-82.79 ± 0.20*
9d + tyloxapol	25	-72.72 ± 0.42*	-73.92 ± 0.21*
	50	-63.99 ± 0.72*	-61.10 ± 0.75*
	100	-62.01 ± 0.39*	-51.36 ± 0.39*

*Significantly different from the tyloxapol group ($p < 0.05$)

^aExpressed as a percentage of the group treated with tyloxapol only (mean ± standar error, $n = 6$)

^b141.16 mmol/L

^c1.26 mmol/L

The best hypolipidemic agents were the acylphenoxacetic esters **5a–c**, depleting cholesterol and triglycerides to almost the same extent as the positive control (simvastatin). A similar result was observed for the analogous series

derived from isovanillin **4a–f** (Mendieta et al. 2014), as well as for the analogs to α -asarone **3a–f** (Mendieta et al. 2014). However, an inverse hypolipidemic effect was found for other homologs structurally closer to α -asarone (Cruz et al. 2001), among which the most potent activity was displayed by those containing an alkyl vs. acyl side chain.

Actually, the alkyl side chain would be expected to act as an important hypocholesterolemic pharmacophore, because of its strong lipophilic binding interaction with the HMGR active site (Argüelles et al. 2010). Nevertheless, there was no relation between the side chain length and the hypocholesterolemic effect, evidenced by the comparable reduction in serum cholesterol values of the homologs in the **5a–c** and **6a–c** series. Regardless of the possible synergetic effect of the acyl and alkyl side chains on the test compounds, the phenoxyacetic ester frame appears to play the main role as the pharmacophore moiety (Table 1), as has been reported (Argüelles et al. 2010; Cruz et al. 2003; Labarrios et al. 1999; Zúñiga et al. 2005; Mendieta et al. 2014).

Interestingly, among the four tested 1,2-dihydroquinolines, **9a**, **9b**, and **9d** displayed high hypocholesterolemic and hypotriglyceridemic activity, which is relevant and almost unique for this kind of heterocycles (Lagu et al. 2007; Matsuda et al. 2007; Guo et al. 2017). The change of substituents in the A ring of the heterocyclic frame does not seem to have a significant influence on the hypolipidemic effect of the compounds, suggesting that the 1,2-dihydroquinoline scaffold could be the active pharmacophore of these potential hypolipidemic agents. Despite the non-significant hypocholesterolemic activity of **9c**, it was able to diminish the level of triglycerides significantly.

Although a dose-response relationship cannot be established for each member of the series, in many cases the 25 mg/kg dose (the closest to that of the control group) produced the greatest effect (Table 1).

Antifungal activity

Statins have been reported to produce in vitro activity against several human pathogenic fungi, including *Candida* spp. and *Aspergillus* spp. (Qiao et al. 2007; Cabral et al. 2013). Hence, the test compounds (except **6c** and **7b**) and itraconazole (the reference) were tested in vitro against four filamentous fungi (*Aspergillus fumigatus* ATCC-16907, *Trichosporon cutaneum* ATCC-28592, *Rhizopus oryzae* ATCC-10329, and *Mucor hiemalis* ATCC-8690) and three yeast specimens (*Candida albicans* ATCC-10231, *C. utilis* ATCC-9226, and *C. tropicalis* ATCC-13803) (Table 2). The MIC values (expressed in $\mu\text{g/mL}$) of all compounds were determined in 96-well plates with 3-(*N*-morpholino)propanesulfonic acid (MOPS) as the buffer. Standardized microbiological methods developed by the CLSI (Fothergill 2012;

Table 2 In vitro antifungal activities of most synthesized compounds (MIC, µg/mL)

Compound	Yeast fungi			Filamentous fungi			
	<i>C. alb.</i>	<i>C. uti.</i>	<i>C. trop.</i>	<i>M. hie.</i>	<i>A. fum.</i>	<i>R. ory.</i>	<i>T. cut.</i>
5a	8	8	4	16	16	16	8
5b	8	8	8	16	16	8	16
5c	2	16	16	16	16	8	16
6a	0.5	8	16	16	16	16	16
6b	0.5	16	16	16	16	1	16
7a	8	16	4	16	16	16	2
7c	4	8	16	16	16	16	16
9a	4	16	16	8	16	8	16
9b	16	16	8	16	16	1	16
9c	4	16	8	16	16	16	16
9d	1	8	16	16	16	16	16
Standard ^a	0.03	0.25	0.06	4	1	1	8

C. alb. *Candida albicans*, *C. uti.* *Candida utilis*, *C. trop.* *Candida tropicalis*, *M. hie* *Mucor hiemalis*, *A. fum* *Aspergillus fumigatus*, *R. ory* *Rhizopus oryzae*, *T. cut* *Trichosporon cutaneum*

^aItraconazole

La Regina et al. 2008; Ramírez-Villalva et al. 2017; García-Vanegas et al. 2019) were employed. The sensitivity of the filamentous microorganisms was determined by the microdilution M38-A method (CLSI 2002; Espinel-Ingroff and Canton 2007a), and that of the yeast fungi with the M27-A3 method (CLSI 2008; Espinel-Ingroff and Cantón 2007b; Pfaller and Diekema 2012).

A good effect was produced against *C. albicans* by **6a** and **6b**, though not as good as the inhibition elicited by itraconazole. Contrarily, a lower antifungal activity was found for **5c** and **9d**. None of the present derivatives were active against the yeast fungi *C. utilis* and *C. tropicalis*. Compared with the effect of itraconazole, only **6b** and **9b** demonstrated good growth inhibition of the filamentous fungus *R. oryzae*, and **5a** and **7a** of *T. cutaneum*.

No structure-activity correlation was detected among the active compounds in regard to the growth inhibition of *C. albicans*. However, homologs **6** (containing C-5 alkyl groups) gave a greater antifungal effect than homologs **5** (with the C-5 acyl moiety). Overall, these results indicate that the presence of the methyl phenoxyacetate and 1,2-dihydroquinoline scaffolds seems to impact antifungal capacity.

Fusariosis is one of the most common infections in humans (Garnica and Nucci 2013; Guarro 2013). *Fusarium oxysporum* is an invasive pathogen known to cause infections like keratitis and onychomycosis in immunocompetent individuals, but in immunocompromised patients the infections are frequently fatal (Garnica and Nucci 2013; Guarro and Gené 1995; Cordoba-Guijarro et al. 2002; Olivares et al. 2005). Although the optimal treatment against fusariosis is unclear, the modestly effective drugs consist of antifungal azoles and amphotericin B. In vitro

data demonstrates general resistance of *Fusarium* to the available antifungal drugs with poor MIC values (Guarro 2013; Cordoba-Guijarro et al. 2002).

Consequently, the series **5–7** and **9** were tested as inhibitors of the mycelial growth of the pathogen *F. oxysporum*, using the agar dilution method and captan as the positive control. Captan, a fungicide utilized in agriculture, cosmetics and pharmaceuticals (U.S. Environmental Protection Agency 1984) inhibits the mycelial growth of *Fusarium* spp. (Türkkan and Erper 2015). According to previous studies, it also increases cell vulnerability to oxidative stress (Moreno-Aliaga et al. 1999; Inoue et al. 2018).

The compounds evaluated induced significant cell growth inhibition, from 72 to 90% for **6a–c**, and 70% for **9a** and **9c** (Fig. 3). Interestingly, the presence of the alkyl side chain of derivatives **6** significantly improved growth inhibition, with **6b** displaying the best result (90%). 1,2-Dihydroquinolines **9a** and **9c** contain either an alkyl side chain or alkyl carboxylate.

Cytotoxic activity

The cytotoxic effect of **5a–b**, **6a–b**, and **9a–c** was determined through the MTT (3-[4,5-dimethylthiazol-2-yl]-2,5-diphenyltetrazolium bromide) cell viability assay with cell lines of human cervical cancer (HeLa), prostate cancer (DU-145), breast cancer (MDA-231) and normal skin keratinocytes (HaCaT) (van Meerloo et al. 2011). Death was observed in up to 90% of the cells exposed to these compounds in concentrations higher than 40 µg/mL. In the MDA-231 and DU-145 cell lines, there was up to 50% cell death at 80–100 µg/mL. HeLa and HaCaT cells showed 100% viability following exposure to the non-active

Fig. 3 Growth inhibition of *F. oxysporum* produced by **5a–c**, **6a–c**, **7a**, **7c**, and **9a–d** (at 10 mM) after 72 h of incubation. Data are expressed as the mean \pm standard deviation ($n = 12$) and are significantly different from the control ($p < 0.05$)

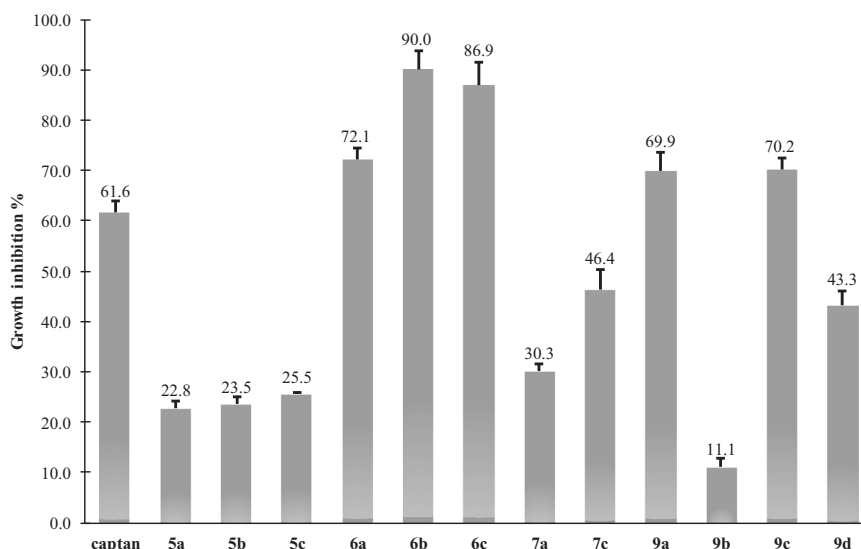


Table 3 Median lethal concentration (LC₅₀) (μg/mL) calculated for derivatives **6a–b** in the four cell lines evaluated

Compound	Cell line/values	MDA-231	DU-145	HeLa	HaCaT ^a
6a	LC ₅₀ (IC 95%)	24 (8–40)	27 (19–35)	44 (25–62)	19 (11–27)
6b	LC ₅₀ (IC 95%)	–	–	73 (60–85)	69 (53–85)
Methotrexate ^b	LC ₅₀ (IC 95%)	>100	>100	>100	>100

A 95% confidential interval (CI 95%) was calculated for each LC₅₀

^aNo tumoral cell line

^bThe reference drug

compounds. In cells incubated exclusively with the vehicle (DMSO), no death occurred, and the decrease in cell growth relative to the control was non-significant.

Only compounds **6a**, **b** exhibited cytotoxicity (Table 3). Derivative **6a** produced an exponential decline in cell viability in all cell lines, including non-tumor cells (HaCaT). Derivative **6b** (at 100 μg/mL) caused greater cytotoxicity in the cervical carcinoma cell line (HeLa) and HaCaT (control) than the other cell lines. Hence the activity of these compounds was non-selective, a characteristic that may be improved by future modifications in their structure. Their selectivity should be thoroughly studied in various cell lines (Xiao et al. 2018) to seek specificity for tumor cells.

Antioxidant activity

Antioxidants are agents capable of protecting a biological target against oxidative stress, DNA mutations and cell damage, helping to prevent many human diseases. For example, oxidative stress plays a pivotal role in the development of diabetes, cancer, and cardiovascular disease (Pisoschi and Pop 2015). The antioxidant potential was herein evaluated for the synthesized compounds for two main reasons that suggest a free radical scavenging capacity of these derivatives. Firstly, alkylphenols **6a–c** are analogs

of α -asarone (**1**), which has antioxidant properties (Pages et al. 2010). Secondly, the 1,2-dihydroquinoline ethoxyquin is a known antioxidant feed additive (Dorey et al. 2000; Błaszczuk and Skolimowski 2007; Błaszczuk et al. 2013; de Koning 2002; Błaszczuk et al. 2006; Błaszczuk and Skolimowski 2005; Błaszczuk and Skolimowski 2006).

The antioxidant activity of the series of analogs **5a–c**, **6a–c**, **7a**, **7c**, and **9a–d** was assessed by using the radical scavenging method with the 2,2-diphenyl-1-picrylhydrazyl radical (DPPH[•]) and 2,2'-azino-bis(3-ethylbenzothiazoline-6-sulphonic acid) radical cation (ABTS^{•+}). Antioxidant activity was expressed as the percentage of decrease in DPPH and ABTS (Table 4). Butylated hydroxytoluene (BHT) was the positive control for the DPPH assay, and the TEAC (mM) was the unit for expressing the data of the ABTS assay (Huang et al. 2005).

The **6a–c** and **9a–d** series showed good radical scavenging capacity in the DPPH assay. The IC₅₀ values for **6a–c** were in a narrow range (0.24–0.25 mM) and for **9a–d** in a much wider range (0.12–1.52 mM). Moreover, a stronger antioxidant effect was detected for **6a–c**, **9a**, and **9c** than BHT (based on the IC₅₀ determination). For **6a–c**, the presence of an alkyl side chain apparently promoted antioxidant activity (Gallardo et al. 2016), while the existence of an acyl group on the side chain notably diminished it.

Table 4 DPPH[•] and ABTS^{•+} cation radical scavenging activity of **5a–c**, **6a–c**, **7a**, **7c**, and **9a–d**^a

Compound	DPPH Scavenging activity		ABTS Scavenging activity	
	% (10 mM)	(IC ₅₀ mM)	% (10 mM)	(mM Trolox/g)
5a	40.6 ± 0.60		13.40 ± 0.20	0.244 ± 0.002
5b	15.9 ± 0.61		11.68 ± 1.38	0.220 ± 0.014
5c	19.1 ± 0.60		13.23 ± 0.71	0.216 ± 0.007
6a	95.3 ± 1.82	0.241 ± 0.009	98.80 ± 0.01	1.509 ± 0.001
6b	94.2 ± 1.50	0.255 ± 0.016	98.61 ± 0.01	1.424 ± 0.001
6c	94.2 ± 1.10	0.244 ± 0.012	98.62 ± 2.39	1.349 ± 0.001
7a	0.2 ± 0.32		0.91 ± 0.37	0.050 ± 0.004
7c	0.9 ± 0.24		0.25 ± 0.48	0.058 ± 0.005
9a	93.5 ± 1.94	0.127 ± 0.030	97.81 ± 3.94	1.552 ± 0.039
9b	93.6 ± 2.49	1.519 ± 0.023	97.53 ± 0.01	1.095 ± 0.001
9c	94.3 ± 1.16	0.238 ± 0.022	98.78 ± 0.01	1.244 ± 0.001
9d	91.0 ± 1.93	1.52 ± 0.015	68.07 ± 0.044	1.00 ± 0.021
BHT	85.02 ± 3.33	0.84 ± 0.08	–	–

^aThe DPPH scavenging activity is calculated as the IC₅₀, and the ABTS scavenging activity as the mM Trolox equivalent (TEAC, mM). Data are expressed as the mean ± standard deviation (*n* = 6), with significant differences considered at *p* < 0.05

This characteristic was not affected by the side chain length. Regarding the 1,2-dihydroquinolines **9a–d**, the presence of a hindered group, such as the phenyl (**9b**) or the cycloalkyl (**9d**) groups, played a negative role, slightly reducing the DPPH[•] scavenging activity (IC₅₀ for both **9b** and **9d** was 1.52 mM). Contrarily, the alkyl (**9a**) and methoxycarbonyl (**9c**) groups improved the antioxidant effect, being almost sevenfold greater with **9a** (IC₅₀ = 0.12 mM) than BHT (IC₅₀ = 0.84 mM). The significant activity of **9a** can be attributed to the lipophilicity of the 2-ethyl and 2-methyl groups (Dorey et al. 2000). Interestingly, the methoxy group attached at either the C-6 or C-7 position of the quinoline ring did not substantially affect the DPPH[•] radical scavenging capacity, although its presence seems to have contributed considerably to the antioxidant effect (Dorey et al. 2000; Błaszczuk and Skolimowski 2007; Błaszczuk et al. 2013; de Koning 2002).

Series **6a–c** and **9a–d** also displayed good ABTS^{•+} radical inhibition (Table 4) with **6a** and **9a** giving the best ABTS^{•+} scavenging capacity (1.51 and 1.55 mM of TEAC). There was a similar pattern for the DPPH[•] radical scavenging activity, finding the best results for **9a** and no effect for compounds **5a–c**, **7a** and **7c**. In summary, the phenoxyacetic ester and 1,2-dihydroquinoline scaffolds demonstrated a significant antioxidant activity, which was improved by the presence of an alkyl side chain or a polar carboxylate group.

Docking of analogs **5**, **6**, and **9** on human HMGR

The in vitro inhibition of HMGRh has been demonstrated for **3** and **4**, showing a significant structure-binding contact similarities with respect to simvastatin (Mendieta et al.

2014). Hence, a docking study was carried out for the most active hypolipidemic derivatives (**5b**, **6a**, **9a**, and **9d**) of the four series herein evaluated.

Docking studies were conducted on Autodock version 4.0 and AutoDockTools (Morris et al. 2009) to explore the binding mode of the test compounds and the reference drug (simvastatin) at the active site of HMGRh (retrieved from the PDB; code: 1HW9) (Istvan and Deisenhofer 2001). The binding energy was calculated and the interaction residues identified in each case (Table 5).

The binding modes of **5b**, **6a**, **9a**, **9d**, and simvastatin (Fig. 4) involve the amino acid side chains of the active site of the enzyme, including Glu559, Arg590, Asp690, Lys691, and Asn755. In a previous study by our group (Mendieta et al. 2014), these residues were identified and Glu559 and Lys691 were found to be the key residues (Andrade-Pavón et al. 2017; Andrade-Pavón et al. 2019). The acylphenoxyacetic ester **5b** had a better binding energy (−7.47 kcal/mol) than the alkylphenoxyacetic ester **6a** (−5.93 kcal/mol). The docking data correlate with the results of the in vivo assessment of their hypolipidemic activity, since **5a–c** decreased the levels of cholesterol and triglycerides to a greater extent than **6a–c**.

Compounds **5b**, **6a**, and simvastatin share key hydrophilic interactions, such as conventional hydrogen and carbon-hydrogen bonding to the active site of the HMGRh enzyme, mainly with amino acid side chains Glu559, Ser684, Asp690, and Lys735. There are some key similarities in the interactions. For instance, the hydroxyl group at C-4 of the aromatic ring of both **5b** and **6a** interact with the same residue (Ser684) as the carboxylate group of simvastatin. Moreover, there is an interaction with Lys735 by

Table 5 Docking results for **5b**, **6a**, **9a**, **9d**, and simvastatin at the active site of HMGRh

Compound	Binding energy ΔG (kcal/mol)	Interacting residues	Polar interactions	Hydrophobic interactions
Simvastatin	-8.45	Glu559, Gly560, Cys561, Leu562, Arg590, Met657, Asn658, Ser661, Ser684, Asn686, Asp690, Lys691, Lys692, Lys735, Ala751, His752, Asn755, Leu853, Leu857	O-H \cdots O (Ser684) O-H \cdots O (Asp690) O-H \cdots O (Ala751) O \cdots H-N (Lys735) O-H \cdots O (Ser684) O \cdots H-N (Lys735) C-H \cdots O (Glu559)	Alkyl (Cys561, Leu562) π -alkyl (His752)
5b	-7.47	Glu559, Leu562, Arg590, Val683, Ser684, Asp690, Lys691, Lys692, Lys735, His752, Asn755, Leu853, Leu857	O-H \cdots O (Ser684) O \cdots H-N (Lys735) O \cdots H-N (Asn755) C-H \cdots O (Glu559) C-H \cdots O (Asp690) C-H \cdots O (Ala751)	π -cation (Arg590) π -sigma (Leu853)
6a	-5.93	Glu559, Arg590, Met657, Ser684, Asp690, Lys691, Lys692, Lys735, Ala751, His752, Asn755, Leu853, Leu857	O-H \cdots O (Ser684) O \cdots H-N (Lys735) O \cdots H-N (Asn755) C-H \cdots O (Glu559) C-H \cdots O (Asp690) C-H \cdots O (Ala751)	Alkyl (Leu857) π -cation (Arg590) π -sigma (Leu853) π -anion (Asp690)
9a	-8.22	Glu559, Arg590, Met657, Val683, Ser684, Asp690, Lys691, Lys692, Ala751, His752, Leu853, Leu857	N-H \cdots O (Asp690) C-H \cdots O (Glu559)	Alkyl (Val683, Leu857) π -cation (Arg590) π -alkyl (Met657)
9d	-8.21	Arg590, Met657, Asn658, Ser661, Ser684, Asp690, Lys691, Lys692, Lys735, Ala751, His752, Asn755, Leu853, Leu857	N-H \cdots O (Asp690) C-H \cdots O (Asp658) C-H \cdots O (Asp661)	Alkyl (Lys691, Leu853, Leu857) π -cation (Arg590) π -alkyl (Met657)

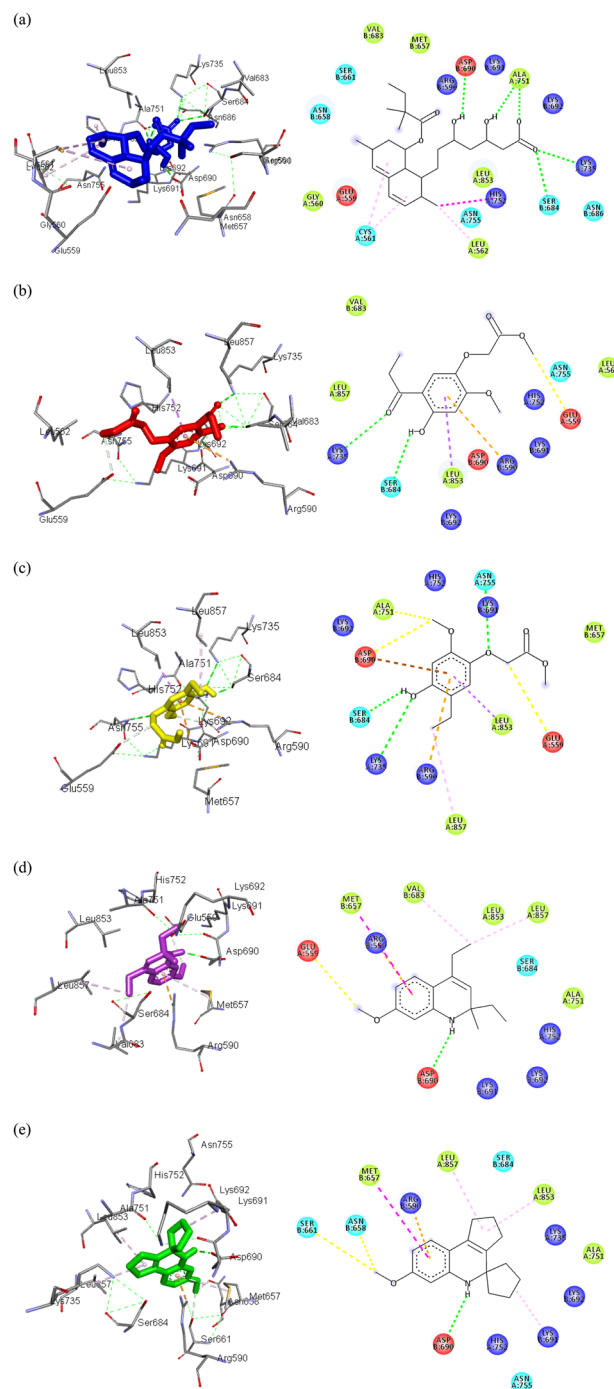
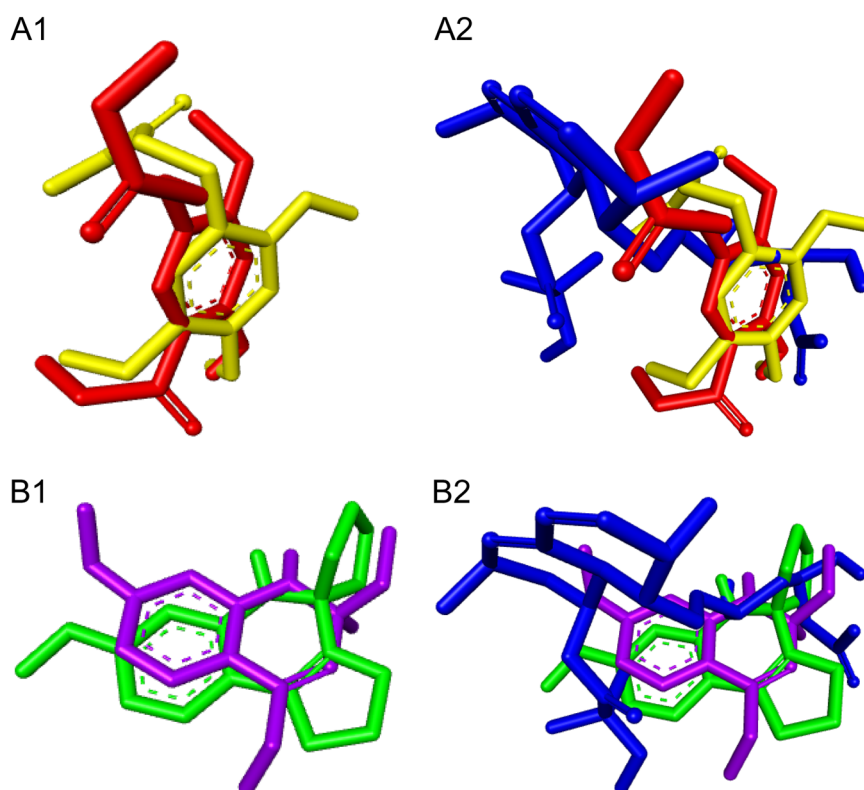
**Fig. 4** Predicted binding mode of simvastatin (**a**), **5b** (**b**), **6a** (**c**), **9a** (**d**), and **9d** (**e**) at the active site of HMGRh (1HW9) using Autodock version 4.0 and AutoDockTools. The 3D model portrays select amino acid residues bound by the ligands at the active site of HMGRh. Only the hydrophilic bonds are shown for better clarity. In the 2D model, the following interactions are denoted with dotted lines: conventional hydrogen bonds (green), carbon-hydrogen (yellow), alkyl (light pink), π -anion (brown), π -cation (orange), π -sigma (purple), and π -alkyl (dark pink). The amino acid residues are illustrated as: hydrophobic (green), polar (cyan), positively charged (blue), and negatively charged (red)

Fig. 5 A1 Overlay of the docking poses of **5b** (red) and **6a** (yellow). B1 Overlay of **9a** (purple) and **9d** (green). A2–B2 The binding mode is compared between the two pairs of compounds and simvastatin (blue)



the hydroxyl group at the C-4 position of **6a**, the carbonyl groups of **5b** and simvastatin. The three compounds also have comparable hydrophobic interactions, such as π -sigma with the amino acid Leu853. Due to their strongly activated aromatic ring, compounds **5b** and **6a** share electrostatic interactions of the π -cation type with the Arg590 residue. The carbonyl oxygen atom of **5b** forms an additional hydrogen bond contact with the side chain of Lys735. This residue may affect the enzymatic activity of **6a** by interacting with the alkyl side chain. The latter observations are in agreement with the *in vivo* assessment of hypolipidemic activity, which was improved by the polar-induced effect of the carbonyl group in the chain.

The results support our hypothesis that by replacing the C-4 methoxy group of **1** by a hydroxyl group, and maintaining a hydrogen bond network comparable to the one existing in **3** and **4**, the hypolipidemic effect of **5b** and **6a** should be conserved.

For 1,2-dihydroquinolines **9a** and **9d**, on the other hand, a very similar binding energy was found (−8.22 and 8.21 kcal/mol, respectively) (Table 5). Furthermore, **9a** had the binding energy closest to the value for simvastatin. It is likely that the hydrocarbon portion present in both **9a**, **9d** and the reference drug enhances the number of the interactions within the active site as well as the overall stability (Figs 4 and 5). In addition, **9a** and **9d** share hydrophilic interactions between their polar NH and the Asp690 residue

of the enzyme, involving conventional hydrogen bonds and carbon-hydrogen bonds. These interactions are comparable to those observed for the acylphenoxyacetic esters **5**, the alkylphenoxyacetic esters **6**, and the hydroxy group of simvastatin. The presence of a high electron density aromatic ring in **9a** and **9d** led to π -cation interactions with Arg590, and to π -alkyl and alkyl interactions with the side chains of Met657 and Leu857, respectively.

Compounds **5b** and **6a** adopt similar orientation at the active site of the enzyme, especially for the activated aromatic ring (Fig. 5). The orientation of 1,2-dihydroquinolines **9a** and **9d** is also alike, mainly due to the benzoheterocyclic frame. They adopt a conformation in which the polar and the hydrophobic functional groups occupy a position similar to some of the groups in simvastatin with comparable polarity, although the structure of the latter is different. Despite this difference, compounds **5b**, **6a**, **9a**, and **9d** interact with most amino acids in the active site of the enzyme that are targeted by the reference drug. Based on the docking data, **5a–c**, **6a–c**, and **9a–d** are likely to have the same mechanism of action as simvastatin.

To the best of our knowledge, there are no reports of molecular docking of 1,2-dihydroquinolines like **9a** and **9d** in the active site of the HMGRh enzyme. The interaction energy calculated from docking was correlated with the *in vivo* hypolipidemic effect.

Conclusions

Most members of the three series of acyl phenols (**5a–c**) and alkyl phenols (**6a–c**) and 1,2-dihydroquinolines (**9a–d**) showed a potent hypolipidemic effect, resulting in an over 67% decrease in serum cholesterol and triglycerides at the lowest doses (25 g/kg). Using the most effective derivatives (**5b**, **6a**, **9a**, and **9d**), docking studies were carried out on human HMGR finding that the different polar and non-polar functional groups of the ligands exhibited strong and multiple interactions with the active site of this enzyme. Hence, the mechanism of action of these compounds probably involves the inhibition of HMGR. However, due to the structural similarity of analogs **5** and **6** with fibrates, the activation of PPAR α cannot be ruled out as a competitive mechanism participating in a reduction of the level of triglycerides.

Regarding antifungal potential, the same three series caused a moderate to robust growth inhibition of *C. albicans*, *R. oryzae*, *T. cutaneum* and *F. oxysporum*, which are highly pathogenic fungi. For the latter fungus, derivatives **6a–c** and **9a** and **9c** proved to be more active than the positive control (captan). On the other hand, derivative **6a** produced cytotoxicity not only in all the cancer cell lines (MDA-231, DU-145 and HeLa) but also in normal cells (HaCaT), indicating a lack of selectivity. Finally, both the **6a–c** and **9a–d** series demonstrated good antioxidant capacity, evidenced by the strong DPPH and ABTS scavenging activity. Indeed, **6a–c** and **9a** and **9c** were more active than the positive control (BHT).

Overall, the phenoxyacetic acid esters derived from vanillin and 1,2-dihydroquinolines showed promise as frames for novel hypolipidemic, antifungal, anticancer and antioxidant agents. Thus, the corresponding structures may be advantageous as templates for the design of new compounds with more potent pharmacological activity.

Acknowledgements We thank Dr Alberto Feliciano and Rsuini U. Gutiérrez for experimental support and Bruce Allan Larsen for proofreading the manuscript. AM, LG-S, MCC-L, FJ, OG-G, LV-T, ER-G, GC-C, FD, and JT gratefully acknowledge the financial support provided by SIP-IPN (grants 20160791, 20170902, 20180198, 20181332, 20181433, 20195228, 20195287, and 20195606) and CONACYT (grants 178319, 282033, CB-283225, A1-S-17131, and 300520). AF-B and CG-R are thankful to the UAEM for funding. MAV gratefully recognized the spectroscopy services provided by the National Laboratory of the Universidad de Guanajuato (UGUAA-CONACYT grant 260373). AP, AM, DAM, RIH-B, LR, CR-E, AR-V, JL, BR-A, and AS-J appreciate the graduate scholarship awarded by CONACYT, as well as the scholarship complements furnished by the SIP-IPN (BEIFI) and the Ludwig K. Hellweg Foundation. LG-S, MCC-L, FJ; LV-T, ER-G, GC-C, FD and JT are fellows of the EDI-IPN and COFAA-IPN programs.

Compliance with ethical standards

Conflict of interest The authors declare that they have no conflict of interest.

Publisher's note Springer Nature remains neutral with regard to jurisdictional claims in published maps and institutional affiliations.

References

- Aguilar-Salinas CA, Olaiz G, Valles V, Ríos-Torres JM, Gómez-Pérez FJ, Rull JA, Franco A, Sepulveda J (2001) High prevalence of low HDL cholesterol concentrations and mixed hyperlipidemia in a Mexican nationwide survey. *J Lipid Res* 42:1298–1307
- Andrade-Pavón D, Cuevas-Hernández RI, Trujillo-Ferrara JG, Hernández-Rodríguez C, Ibarra JA, Villa-Tanaca L (2017) Recombinant 3-hydroxy 3-methyl glutaryl-CoA reductase from *Candida glabrata* (Rec-CgHMGR) obtained by heterologous expression, as a novel therapeutic target model for testing synthetic drugs. *Appl Biochem Biotechnol* 182:1478–1490
- Andrade-Pavón D, Ortiz-Álvarez J, Sánchez-Sandoval E, Tamariz J, Hernández-Rodríguez C, Ibarra JA, Villa-Tanaca L (2019) Inhibition of recombinant enzyme 3-hydroxy-3-methylglutaryl-CoA reductase from *Candida glabrata* by α -asarone-based synthetic compounds as antifungal agents. *J Biotechnol* 292:64–67
- Argüelles N, Sánchez-Sandoval E, Mendieta A, Villa-Tanaca L, Garduño-Siciliano L, Jiménez F, Cruz MC, Medina-Franco JL, Chamorro-Cevallos G, Tamariz J (2010) Design, synthesis, and docking of highly hypolipidemic agents: *Schizosaccharomyces pombe* as a new model for evaluating α -asarone-based HMG CoA inhibitors. *Bioorg Med Chem* 18:4238–4248
- BIP study group (2000) Secondary prevention by raising HDL cholesterol and reducing triglycerides in patients with coronary artery disease. The bezafibrate infarction prevention (BIP) study. *Circulation* 102:21–27
- Błaszczuk A, Augustyniak A, Skolimowski J (2013) Ethoxyquin: an antioxidant used in animal feed. *Int J Food Sci* 2013:585931
- Błaszczuk A, Skolimowski J (2005) Apoptosis and cytotoxicity caused by ethoxyquin and two of its salts. *Cell Mol Biol Lett* 10:15–21
- Błaszczuk A, Skolimowski J (2006) Comparative analysis of cytotoxic, genotoxic and antioxidant effects of 2,2,4,7-tetramethyl-1,2,3,4-tetrahydroquinoline and ethoxyquin on human lymphocytes. *Chem-Biol Interact* 162:70–80
- Błaszczuk A, Skolimowski J (2007) Preparation of ethoxyquin salts and their genotoxic and antioxidant effects on human lymphocytes. *Arkivoc* vi:217–229
- Błaszczuk A, Skolimowski J, Materac A (2006) Genotoxic and antioxidant activities of ethoxyquin salts evaluated by the comet assay. *Chem-Biol Interact* 162:268–273
- Bradfute DL, Simoni RD (1994) Non-sterol compounds that regulate cholesterologenesis. Analogues of farnesyl pyrophosphate reduce 3-hydroxy-3-methylglutaryl-coenzyme A reductase levels. *J Biol Chem* 269:6645–6650
- Brown JW, Gangloff AR, Jennings AJ, Vu PH (2010) Poly (ADP-ribose) polymerase (PARP) inhibitors. Patent WO 2010/111626 A2
- Cabral ME, Figueroa LIC, Fariña JI (2013) Synergistic antifungal activity of statin-azole associations as witnessed by *Saccharomyces cerevisiae*- and *Candida utilis*-bioassays and ergosterol quantification. *Rev Iberoam Micol* 30:31–38
- Campos-Ríos MG, Chiang Cabrera F (2006) Una revisión nomenclatural de los tipos de plantas de la península de Yucatán (México). *Polibotánica* 89–149

- Cevallos-Casals BA, Cisneros-Zevallos L (2003) Stoichiometric and kinetic studies of phenolic antioxidants from Andean purple corn and red-fleshed sweetpotato. *J Agric Food Chem* 51:3313–3319
- Chalasanani N (2005) Statins and hepatotoxicity: focus on patients with fatty liver. *Hepatology* 41:690–695
- Chamorro G, Salazar M, Salazar S, Mendoza T (1993) Farmacología y toxicología de *Guatteria gaumeri* y alfa-asarona. *Rev Invest Clin* 45:597–604
- Chander S, Ashok P, Zheng Y-T, Wang P, Raja KS, Taneja A, Murugesan S (2016a) Design, synthesis, and in-vitro evaluation of novel tetrahydroquinoline carbamates as HIV-1 RT inhibitor and their antifungal activity. *Bioorg Chem* 64:66–73
- Chander S, Wang P, Ashok P, Yang L-M, Zheng Y-T, Murugesan S (2016b) Rational design, synthesis, anti-HIV-1 RT and antimicrobial activity of novel 3-(6-methoxy-3,4-dihydroquinolin-1(2H)-yl)-1-(piperazin-1-yl)propan-1-one derivatives. *Bioorg Chem* 67:75–83
- Chung MC, Bosquesi PL, dos Santos JL (2011) A prodrug approach to improve the physico-chemical properties and decrease the genotoxicity of nitro compounds. *Curr Pharm Des* 17:3515–3526
- Clinical and Laboratory Standards Institute (CLSI) (2002) Document M38-A2: reference method for broth dilution antifungal susceptibility testing of filamentous fungi, 2nd edn. Approved Standard, Clinical and Laboratory Standards Institute, Wayne, PA
- Clinical and Laboratory Standards Institute (CLSI) (2008) M27-A3: reference Method for broth dilution antifungal susceptibility testing of yeasts, 3rd edn. Approved Standard, Clinical and Laboratory Standards Institute, Wayne, PA
- Cordoba-Guijarro S, Ruiz-Rodríguez R, Acevedo-Barberá A, Serrano-Pardo R (2002) Disseminated fusarium infection in a patient with acute myelogenous leukemia. *Actas Dermo-Sifiliogr* 93:118–121
- Cruz MC, Salazar M, Garcíafigueroa Y, Hernández D, Díaz F, Chamorro G, Tamariz J (2003) Hypolipidemic activity of new phenoxycetic derivatives related to α -asarone with minimal pharmacophore features. *Drug Dev Res* 60:186–195
- Cruz A, Garduño L, Salazar M, Martínez E, Jiménez-Vázquez HA, Díaz F, Chamorro G, Tamariz J (2001) Synthesis and hypolipidemic activity of modified side chain α -asarone homologues. *Arznei-Forsch/Drug Res* 51:535–544
- Dassault Systèmes (2016) BIOVIA, discovery studio modeling environment; release 2017. Dassault Systèmes, San Diego, CA
- Davidson MH, Armani A, McKenney JM, Jacobson TA (2007) Safety considerations with fibrate therapy. *Am J Cardiol* 99:S3–S18
- de Koning AJ (2002) The antioxidant ethoxyquin and its analogues: a review. *Int J Food Prop* 5:451–461
- Dorey G, Lockhart B, Lestage P, Casara P (2000) New quinolinic derivatives as centrally active antioxidants. *Bioorg Med Chem Lett* 10:935–939
- Edelstein C, Byrne RE, Yamamoto K, Zarins C, Scanu AM (1985) Plasma lipoprotein changes attending the intravenous administration of Triton WR-1339 in normolipidemic dogs: preferential effect on high density lipoproteins. *J Lipid Res* 26:351–359
- Elisaf MS, Florentin M, Liberopoulos EN, Mikhailidis DP (2008) Fibrate-associated adverse effects beyond muscle and liver toxicity. *Curr Pharm Des* 14:574–587
- Espinell-Ingroff A, Canton E (2007a) Antifungal susceptibility testing of filamentous fungi. In: Schwalbe R, Steele-Moore L, Goodwin AC (eds) Antimicrobial susceptibility testing protocols. CRC Press, Florida, p 209–241
- Espinell-Ingroff A, Cantón E (2007b) Antifungal susceptibility testing of yeasts. In: Schwalbe R, Steele-Moore L, Goodwin AC (eds) Antimicrobial susceptibility testing protocols. CRC Press, Florida, p 173–208
- Fazio S, Linton MF (2004) The role of fibrates in managing hyperlipidemia: mechanisms of action and clinical efficacy. *Curr Atheroscler Rep*. 6:148–157
- Field FJ, Born E, Mathur SN (1997) Effect of micellar α -sitosterol on cholesterol metabolism in CaCo-2 cells. *J Lipid Res* 38:348
- Fothergill AW (2012) Antifungal susceptibility testing: Clinical Laboratory and Standards Institute (CLSI) methods. In: Hall GS (ed) Interactions of yeasts, moulds, and antifungal agents. How to detect resistance. Springer Science-Business Media, Berlin, p 65–74
- Freshney RI (2010) Define media and supplements. In: Culture of animal cells, chap. 8. Wiley-Blackwell, Hoboken, NJ, p 99–114
- Frisch MJ, Trucks GW, Schlegel HB, Scuseria GE, Robb MA, Cheeseman JR, Montgomery Jr JA, Vreven T, Kudin KN, Burant JC, Millam JM, Iyengar SS, Tomasi J, Barone V, Mennucci B, Cossi M, Scalmani G, Rega N, Petersson GA, Nakatsuji H, Hada M, Ehara M, Toyota K, Fukuda R, Hasegawa J, Ishida M, Nakajima T, Honda Y, Kitao O, Nakai H, Klene M, Li X, Knox JE, Hratchian HP, Cross JB, Bakken V, Adamo C, Jaramillo J, Gomperts R, Stratmann RE, Yazyev O, Austin AJ, Cammi R, Pomelli C, Ochterski JW, Ayala PY, Morokuma K, Voth GA, Salvador P, Dannenberg JJ, Zakrzewski VG, Dapprich S, Daniels AD, Strain MC, Farkas O, Malick DK, Rabuck AD, Raghavachari K, Foresman JB, Ortiz JV, Cui Q, Baboul AG, Clifford S, Cioslowski J, Stefanov BB, Liu G, Liashenko A, Piskorz P, Komaromi I, Martin RL, Fox DJ, Keith T, Al-Laham MA, Peng CY, Nanayakkara A, Challacombe M, Gill PMW, Johnson B, Chen W, Wong MW, Gonzalez C, Pople JA (2004) Gaussian 98 Inc., Version A.6, Wallingford, CT
- Gallardo E, Palma-Valdés R, Sarriá B, Gallardo I, de la Cruz JP, Bravo L, Mateos R, Espartero JL (2016) Synthesis and antioxidant activity of alkyl nitro derivatives of hydroxytyrosol. *Molecules* 21:E656
- García-Vanegas JJ, Ramírez-Villalva A, Fuentes-Benites A, Martínez-Otero D, González-Rivas N, Cuevas-Yañez E (2019) Synthesis and in-vitro biological evaluation of 1,1-diaryl-2-(1,2,3)triazol-1-yl-ethanol derivatives as antifungal compounds flutriafol analogues. *J Chem Sci* 131:27
- Garnica M, Nucci M (2013) Epidemiology of fusariosis. *Curr Fungal Infect Rep*. 7:301–305
- Gielen S, Sandri M, Schuler G, Teupser D (2009) Risk factor management: antiatherogenic therapies. *Eur J Cardiovasc Prev Rehabil* 16:S29–S36
- Goldfard S (1978) Rapid increase in hepatic HMG CoA reductase activity and in vivo cholesterol synthesis after Triton WR 1339 injection. *J Lipid Res* 19:489–494
- Golomb BA, Evans MA (2008) Statin adverse effects: a review of the literature and evidence for a mitochondrial mechanism. *Am J Cardiovasc Drugs* 8:373–418
- Graham DJ, Staffa JA, Shatin D, Andrade SE, Schech SD, La Grenade L, Gurwitz JH, Chan KA, Goodman MJ, Platt RP (2004) Incidence of hospitalized rhabdomyolysis in patients treated with lipid-lowering drugs. *JAMA* 292:2585–2590
- Grenier JL, Cotelle N, Catteau JP, Cotelle P (2000) Synthesis and physico-chemical properties of nitrocafeic acids. *J Phys Org Chem* 13:511–517
- Grundy SM, Cleeman JI, Daniels SR, Donato KA, Eckel RH, Franklin BA, Gordon DJ, Krauss RM, Savage PJ, Smith Jr SC, Spertus JA, Costa F (2005) Diagnosis and management of the metabolic syndrome. An American Heart Association/National Heart, Lung, and Blood Institute Scientific Statement. *Circulation* 112:2735–2752
- Guarro J (2013) Fusariosis, a complex infection caused by a high diversity of fungal species refractory to treatment. *Eur J Clin Microbiol Infect Dis* 32:1491–1500
- Guarro J, Gené J (1995) Opportunistic fusarial infections in humans. *Eur J Clin Microbiol Infect Dis* 14:741–754
- Guo F, Li Y, Zhao Y, Yi J, Huang C (2017) Dihydroquinolinone compound with PPAR multiple agonist activity, preparation and

- application for preventing and/or treating metabolic syndrome. Patent N° CN 107522657 A 20171229
- Gutiérrez RU, Correa HC, Bautista R, Vargas JL, Jerezano AV, Delgado F, Tamariz J (2013) Regioselective synthesis of 1,2-dihydroquinolines by a solvent-free MgBr₂-catalyzed multicomponent reaction. *J Org Chem* 78:9614–9626
- Haines BE, Wiest O, Stauffacher CV (2013) The increasingly complex mechanism of HMG-CoA reductase. *Acc Chem Res* 46:2416–2426
- Harada-Shiba M, Tajima S, Yamamoto A (1995) Response of 3-hydroxy-3-methylglutaryl CoA reductase to *l*-triiodothyronine in cultured fibroblasts from FH homozygotes. *Atherosclerosis* 113:91–98
- Hegedüs A, Hell Z, Vargadi T, Potor A, Gresits I (2007) A new, simple synthesis of 1,2-dihydroquinolines via cyclocondensation using zeolite catalyst. *Catal Lett* 117:99–101
- Hodel C (2002) Myopathy and rhabdomyolysis with lipid-lowering drugs. *Toxicol Lett* 128:159–168
- Huang D, Ou B, Prior RL (2005) The chemistry behind antioxidant capacity assays. *J Agric Food Chem* 53:1841–1856
- Inoue T, Kinoshita M, Oyama K, Kamemura N, Oyama Y (2018) Captan-induced increase in the concentrations of intracellular Ca²⁺ and Zn²⁺ and its correlation with oxidative stress in rat thymic lymphocytes. *Environ Toxicol Pharm* 63:78–83
- Irwin JJ, Shoichet BK (2005) ZINC—A free database of commercially available compounds for virtual screening. *J Chem Inf Model* 45:177–182
- Istvan ES, Deisenhofer J (2001) Structural mechanism for statin inhibition of HMG-CoA reductase. *Science* 292:1160–1164
- Johnson JV, Rauckman BS, Baccanari DP, Roth B (1989) 2,4-Diamino-5-benzylpyrimidines and analogues as antibacterial agents. 12. 1,2-Dihydroquinolylmethyl analogues with high activity and specificity for bacterial dihydrofolate reductase. *J Med Chem* 32:1942–1949
- Jover-Fernández A, Hernández-Mijares A (2012) Fibratos: efectos farmacológicos. *Clín Inv Arterioscler* 24(S1):19–23
- Joy TR, Hegele RA (2009) Narrative review: statin-related myopathy. *Ann Intern Med* 150:858–868
- Kiss LE, Ferreira HS, Torrão L, Bonifácio MJ, Palma PN, Soares-da-Silva P, Learmonth DA (2010) Discovery of a long-acting, peripherally selective inhibitor of catechol-*O*-methyltransferase. *J Med Chem* 53:3396–3411
- Korolenko TA, Tuzikov FV, Vasil'eva ED, Cherkanova MS, Tuzikova NA (2010) Fractional composition of blood serum lipoproteins in mice and rats with Triton WR 1339-induced lipemia. *Bull Exp Biol Med* 149:567–570
- Kourounakis AP, Victoratos P, Peroulis N, Stefanou N, Yiangou M, Hadjipetrou L, Kourounakis PN (2002) Experimental hyperlipidemia and the effect of NSAIDs. *Exp Mol Pathol* 73:135–138
- Kuroda M, Tanzawa K, Tsujita Y, Endo A (1977) Mechanism for elevation of hepatic cholesterol synthesis and serum cholesterol levels in Triton WR-1339-induced hyperlipidemia. *Biochim Biophys Acta* 489:119–125
- Labarrios F, Garduño L, Vidal MR, García R, Salazar M, Martínez E, Díaz F, Chamorro G, Tamariz J (1999) Synthesis and hypolipidaemic evaluation of a series of α -asarone analogues related to clofibrate in mice. *J Pharm Pharm* 51:1–7
- Lagu B, Lebedev R, Pio B, Yang M, Pelton PD (2007) Dihydro-[1H]-quinolin-2-ones as retinoid X receptor (RXR) agonists for potential treatment of dyslipidemia. *Bioorg Med Chem Lett* 17:3491–3496
- Lalitha MK (2004) Manual on antimicrobial susceptibility testing (under the auspices of Indian Association of Medical Microbiologists). https://www.biodiamed.gr/wp-content/uploads/2017/06/Manual_on_Antimicrobial_Susceptibility_Testing.pdf Accessed 21 Sept 2004
- Lalloyer F, Staels B (2010) Fibrates, glitazones, and peroxisome proliferator-activated receptors. *Arterioscler Thromb Vasc Biol* 30:894–899
- La Regina G, D'Auria FD, Tafi A, Piscitelli F, Olla S, Caporuscio F, Nencioni L, Cirilli R, La Torre F, Rodrigues De Melo N, Kelly SL, Lamb DC, Artico M, Botta M, Palamara AT, Silvestri R (2008) 1-[(3-Aryloxy-3-aryl)propyl]-1H-imidazoles, new imidazoles with potent activity against *Candida albicans* and dermatophytes. Synthesis, structure-activity relationship, and molecular modeling studies *J Med Chem* 51:3481–3855
- Lee JY, Lee JY, Yun B-S, Hwang BK (2004) Antifungal activity of β -asarone from rhizomes *Acorus gramineus*. *J Agric Food Chem* 52:776–780
- Levine S, Saltzman A (2007) A procedure for inducing sustained hyperlipemia in rats by administration of a surfactant. *J Pharm Toxicol Methods* 55:224–226
- Liu L, Yeh Y-Y (2002) *S*-Alk(en)yl cysteines of garlic inhibit cholesterol synthesis by deactivating HMG-CoA reductase in cultured rat hepatocytes. *J Nutr* 132:1129–1134
- Man RYK, Lynn EG, Cheung F, Tsang PSY, O K (2002) Cholestin inhibits cholesterol synthesis and secretion in hepatic cells (HepG2). *Mol Cell Biochem* 233:153–158
- Maron DJ, Fazio S, Linton MF (2000) Current perspectives of statins. *Circulation* 101:207–213
- Matsuda M, Mori T, Kawashima K, Nagatsuka M, Kobayashi S, Yamamoto M, Kato M, Takai M, Oda T (2007) Preparation of novel 1,2-dihydroquinoline derivatives having glucocorticoid receptor binding activity. *PCT Int Appl WO 2007032556:A1* 20070322
- Medina-Franco JL, López-Vallejo F, Rodríguez-Morales S, Castillo R, Chamorro G, Tamariz J (2005) Molecular docking of the highly hypolipidemic agent α -asarone with the catalytic portion of HMG-CoA reductase. *Bioorg Med Chem Lett* 15:989–994
- Mehta PK, Wei J, Wenger NK (2014) Ischemic heart disease in women: a focus or risk factor. *Trends Cardiovasc Med* 24:140–151
- Mendieta A, Jiménez F, Garduño-Siciliano L, Mojica-Villegas A, Rosales-Acosta B, Villa-Tanaca L, Chamorro-Cevallos G, Medina-Franco JL, Meurice N, Gutiérrez RU, Montiel LE, Cruz MC, Tamariz J (2014) Synthesis and highly potent hypolipidemic activity of alpha-asarone- and fibrate-based 2-acyl and 2-alkyl phenols as HMG-CoA reductase inhibitors. *Bioorg Med Chem* 22:5871–5882
- Menéndez R, Amor AM, Rodeiro I, González RM, González PC, Alfonso JL, Más R (2001) Policosanol modulates HMG-CoA reductase activity in cultured fibroblasts. *Arch Med Res* 32:8–12
- Miyazaki A, Koieyama T, Shimada Y, Kikuchi T, Ito K, Kasanuki N, Koga T (2004) Pravastatin sodium, an inhibitor of HMG-CoA reductase, decreases HDL cholesterol by transfer of cholesteryl ester from HDL to VLDL in Japanese white rabbits. *J Atheroscler Thromb* 11:22–28
- Mohammadzadeh A, Farhat AS, Esmaeli H, Amiri R (2013) Effect of clofibrate on serum triglyceride and cholesterol after intravenous lipid in very low birth weight neonates. *Iran J Neonatol* 4:20–25
- Momin RA, Nair MG (2002) Pest-managing efficacy of *trans*-asarone isolated from *Daucus carota* L. seeds. *J Agric Food Chem* 50:4475–4478
- Moreno-Aliaga MJ, Arenas-Vidal JC, Berjón A, Fernández-Otero MP (1999) Effects of in vivo captan administration on cytotoxicity, gluconeogenesis, ATP levels, and parameters related to oxidative stress in rat liver. *Pest Biochem Physiol* 64:185–193
- Morris GM, Huey R, Lindstrom W, Sanner MF, Belew RK, Goodsell DS, Olson AJ (2009) AutoDock4 and AutoDockTools4: automated docking with selective receptor flexibility. *J Comput Chem* 30:2785–2791

- Motulsky HJ (1999) Analyzing data with GraphPad Prism. GraphPad Prism Software Inc., San Diego, CA. www.graphpad.com
- Okopień B, Buldak Ł, Bóldys A (2018) Benefits and risks of the treatment with fibrates—a comprehensive summary. *Expert Rev Clin Pharm* 11:1099–1112
- Oleander D, Żwawiak J, Zaprutko L (2018) Multidirectional efficacy of biologically active nitro compounds included in medicines. *Pharmaceuticals* 11:54
- Olivares CR, Alfaro LLJ, Diaz JMC, Thompson ML (2005) Disseminated fusariosis by *Fusarium oxysporum* in an adult patient with acute myeloid leukemia and severe febrile neutropenia. *Rev Chil Infect* 22:356–360
- Oliver M (2012) The clofibrate saga: a retrospective commentary. *Br J Clin Pharm* 74:907–910
- Pages N, Maurois P, Delplanque B, Bac P, Stables JP, Tamariz J, Chamorro G, Vamecq J (2010) Activities of α -asarone in various animal seizure models and in biochemical assays might be essentially accounted for by antioxidant properties. *Neurosci Res* 68:337–344
- Panini SR, Sexton RC, Gupta AK, Parish EJ, Chitrakorn S, Rudney H (1986) Regulation of 3-hydroxy-3-methylglutaryl coenzyme A reductase activity and cholesterol biosynthesis by oxysterols. *J Lipid Res* 27:1190
- Parker RA, Pearce BC, Clark RW, Gordon DA, Wright JJK (1993) Tocotrienols regulate cholesterol production in mammalian cells by post-transcriptional suppression of 3-hydroxy-3-methylglutaryl-coenzyme A reductase. *J Biol Chem* 268:11230–11238
- Pfaller MA, Diekema DJ (2012) Progress in antifungal susceptibility testing of *Candida* spp. by use of Clinical and Laboratory Standards Institute broth microdilution methods, 2010 to 2012. *J Clin Microbiol* 50:2846–2856
- Pisoschi AM, Pop A (2015) The role of antioxidants in the chemistry of oxidative stress: a review. *Eur J Med Chem* 97:55–74
- Poplawsky J, Lozowicka B, Dubis AT, Lachowska B, Witkowski S, Siluk D, Petrusiewicz J, Kalisz R, Cybulski J, Strzalkowska M, Chilmonczyk Z (2000) Synthesis and hypolipidemic and antiplatelet activities of α -asarone isomers in humans (in vitro), mice (in vivo), and rats (in vivo). *J Med Chem* 43:3671–3676
- Qiao J, Kontoyiannis DP, Wan Z, Li R, Liu W (2007) Antifungal activity of statins against *Aspergillus* species. *Med Mycol* 45:589–593
- Raju J, Bird RP (2007) Diosgenin, a naturally occurring furostanol saponin suppresses 3-hydroxy-3-methylglutaryl CoA reductase expression and induces apoptosis in HCT-116 human colon carcinoma cells. *Cancer Lett* 255:194–204
- Ramírez-Villalva A, González-Calderón D, Rojas-García RI, González-Romero C, Tamariz-Mascarúa J, Morales-Rodríguez M, Zavala-Segovia N, Fuentes-Benites A (2017) Synthesis and antifungal activity of novel oxazolidin-2-one-linked 1,2,3-triazole derivatives. *Med Chem Commun* 8:2258–2262
- Rashid M, Khan R, Khan RA (2018) Microwave assisted catalytic region-selective nitration of resorcinol and substituted phenols. *Chem Res J* 3:17–24
- Rodríguez-Páez L, Juárez-Sánchez M, Antúnez-Solis J, Baeza I, Wong C (2003) α -Asarone inhibits HMG-CoA reductase, lowers serum LDL-cholesterol levels and reduces biliary CSI in hypercholesterolemic rats. *Phytomedicine* 10:397–404
- Rotta-Bonfin M, Bulle-Oliveira AS, do Amaral SL, Luiz-Monteiro H (2015) Treatment of dyslipidemia with statins and physical exercises: recent findings of skeletal muscle responses. *Arq Bras Cardiol* 104:324–332
- SAS Institute Inc (9.0) (2014) SAS/ACCESS® 9.0, Cary: NC. https://www.sas.com/search/en_us.html?q=SAS/ACCESS%209.0
- Schoonjans K, Peinado-Onsurbe J, Lefebvre A-M, Heyman RA, Briggs M, Deeb S, Staels B, Auwerx J (1996) PPAR α and PPAR γ activators direct a distinct tissue-specific transcriptional response via a PPRE in the lipoprotein lipase gene. *EMBO J* 15:5336–5348
- Shaheen B, Barathi K, Prasad KVSRG (2016) Mini review on therapeutic profile of phenoxy acids and their derivatives. *Int J Pharm Pharm Sci* 8:66–71
- Shaikh SR, Ali SA (2018) Pleiotropic actions of PPAR agonist: a potential therapeutic perspectives in the treatment of diabetic nephropathy. *Innov Pharm Pharmacoth* 6:6–12
- Silva RM, Santos FA, Maciel MAM, Pinto AC, Rao VSN (2001) Effect of *trans*-dehydrocrotonin, a 19-nor-clerodane diterpene from *Croton cajucara* on experimental hypertriglyceridaemia and hypercholesterolaemia induced by Triton WR 1339 (tyloxapol) in mice. *Planta Med* 67:763–765
- Singh N, Tamariz J, Chamorro G, Medina-Franco JL (2009) Inhibitors of HMG-CoA reductase: current and future prospects. *Mini-Rev Med Chem* 9:1272–1283
- Steinberg D (2005) Hypercholesterolemia and inflammation in atherogenesis: two sides of the same coin. *Molec Nutr Food Res* 49:995–998
- Sung JH, Lee S-J, Park KH, Moon TW (2004) Isoflavones inhibit 3-hydroxy-3-methylglutaryl coenzyme A reductase in vitro. *Biosci Biotechnol Biochem* 68:428–432
- Thagizadeh E, Esfehiani RJ, Sahebkar A, Parizadeh SM, Rostami D, Mirinezhad M, Poursheikhani A, Mobarhan MG, Pasdar A (2019) Familial combined hyperlipidemia: an overview of the underlying molecular mechanisms and therapeutic strategies. *IUBMB Life*. <https://doi.org/10.1002/iub.2073>
- The Field Study Investigators (2005) Effects of long-term fenofibrate therapy on cardiovascular events in 9795 people with type 2 diabetes mellitus (the FIELD study): randomised controlled trial. *Lancet* 366:1849–1861
- Trzaskos JM, Magolda RL, Favata MF, Fischer RT, Johnson PR, Chen HW, Ko SS, Leonard DA, Gaylor JL (1993) Modulation of 3-hydroxy-3-methylglutaryl-CoA reductase by 15 α -fluorolanost-7-en-3 β -ol. *J Biol Chem* 268:22591–22599
- Türkkan M, Erper I (2015) Inhibitory influence of organic and inorganic sodium salts and synthetic fungicides against bean root rot pathogens. *Gesund Pflanz* 67:83–94
- Uchida A, Slipchenko MN, Cheng J-X, Buhman KK (2011) Fenofibrate, a peroxisome proliferator-activated receptor α agonist, alters triglyceride metabolism in enterocytes of mice. *Biochim Biophys Acta* 1811:170–176
- U.S. Environmental Protection Agency (1984) Health and environmental effects profile for captan. EPA/600/x-84/253. Environmental Criteria and Assessment Office, Office of Health and Environmental Assessment, Office of Research and Development, Cincinnati, OH
- Van Gaal LF, Mertens IL, De Block CE (2006) Mechanisms linking obesity with cardiovascular disease. *Nature* 444:875–880
- van Meerloo J, Kaspers GJ, Cloos J (2011) Cells sensitivity assays: the MTT assay. *Methods Mol Biol* 731:237–245
- Veseli BE, Perrotta P, De Meyer GRA, Roth L, Van der Donckt C, Martinet W, De Meyer GRY (2017) Animal models of atherosclerosis. *Eur J Pharm* 816:3–13
- Vivancos J, León-Colombo T, Monforte-Dupret C (1999) Hypolipidemic treatment in the prevention of atherosclerotic plaque complications. *Rev Neurol* 29:857–863
- Wierzbicki AS (2001) Atorvastatin. *Expert Opin Pharmacother* 2:819–830
- Williams D, Feely J (2002) Pharmacokinetic–pharmacodynamic drug interactions with HMG-CoA reductase inhibitors. *Clin Pharmacokinet* 41:343–370
- Willson TM, Brown PJ, Stembach DD, Henke BR (2000) The PPARs: from orphan receptors to drug discovery. *J Med Chem* 43:527–550
- Xiao Z, Fei L, Chen X, Wang X, Cao L, Ye K, Zhu W, Xu S (2018) Design, synthesis, and antitumor evaluation of quinoline-imidazole derivatives. *Arch Pharm Chem Life Sci* 351:e1700407

- Yuan G, Al-Shali KZ, Hegele RA (2007) Hypertriglyceridemia: its etiology, effects and treatment. *Can Med Assoc J* 176:1113–1120
- Zeniya M, Reuben A (1988) Triton WR-1339-induced changes in serum lipids and biliary lipid secretion. *Am J Physiol* 254:G346–G354
- Zhang Y, Fang Y, Liang H, Wang H, Hu K, Liu X, Yi X, Peng Y (2013) Synthesis and antioxidant activities of 2-oxo-quinoline-3-carbaldehyde Schiff-base derivatives. *Bioorg Med Chem Lett* 23:107–111
- Zúñiga C, Garduño L, Cruz MC, Salazar M, Pérez-Pastén R, Chamorro G, Labarrios F, Tamariz J (2005) Design of new potent hypolipidemic agents with the synergistic structural properties of α -asarone and fibrates. *Drug Dev Res* 64:28–40